Metal-coordinated networks from metalized porphyrin derivatives and Co adatoms on Ag(111)

A bachelor research project

Author: Michiel Veen
Date: 11th of July 2014
Daily supervisor: F. Studener
First examiner: Dr. M. Stöhr
Second examiner: Dr. R. Tobey

The focus of this project is the deposition of a metalized porphyrin derivative molecule. Firstly the molecule, called Ni-AN153, was deposited on Ag(111). Secondly a additional cobalt deposition was done and thirdly the sample was annealed. The resulting networks where investigated using STM and XPS. The different phases, a close packed and 3-fold hexagonal network, seemed similar to phases seemed found for non-metallic AN153. The latter phase was different from the one found in previous research.

Contents

1) Introduction 3

2) Experimental Techniques 4

2.1) Environmental factors: temperature and vacuum level 4

2.1.1) Bake-out 5

2.2) Sample preparation 5

2.2.1) Degassing 6

2.2.2) Sputtering and annealing 7

2.2.3) Molecule deposition 7

2.3) STM 8

2.3.1) Theoretical background 8

2.3.2) Instrumentation 9

2.3.3) STM measurement modes 10

2.3.4) Vibration isolation 11

2.4) XPS 11

3) Results 12

3.1) STM data of Ni-AN153 on Ag(111) 12

3.2) STM data of Ni-AN153 on Ag(111) after cobalt deposition 16

3.3) XPS data of nickel in Ni-AN153+Co on Ag(111) 22

3.4) XPS data of cobalt in Ni-AN153+Co on Ag(111) 24

4) Discussion 25

4.1) Comparable STM study 25

4.2) Binding motifs of the porphyrin assemblies 28

4.3) XPS analysis 31

4.3.1) Nickel $2p_{3/2}$ 31

4.3.2) Cobalt $2p_{3/2}$ 31

5) Conclusion 32

6) List of abbreviations 32

7) References 33

1) Introduction

Since ancient times surface deposition techniques have been a field of research. For example tinned surfaces are already encountered on bronze age swords[1]. The current field of research, modern surface science, really started to expand with the invention of the scanning tunneling microscope (STM) by Binnig and Rohrer in 1986[2]. The STM is a non-optic scanning microscope which allows imaging and manipulation of individual adsorbed molecules[3] (see the STM chapter under Experimental techniques for more information). After this invention the research in molecular self-assembly took a rise from a few papers in 1991 to around 200 publications in 2007[4]. The main focus of this research is the deposition and self-assembly of molecules on atomically flat surfaces with the ultimate goal of creating functional nanosystems[4]. A promising field of research is the deposition of molecules with ligands able to stabilize networks via metal-organic binding: these molecules can be used to recognize and adsorb specific metals. This selectivity allows for the self-assembly of diverse supramolecular structures[5]. One group of these structures are porous metal organic structures. These structures can be used to arrange metal atoms in well divined guest structures.

This project focuses on such a structure consisting of a organic molecule based on a porphyrin core and nickel and cobalt guest atoms to inhabit this molecule. Porphyrins are a group of organic molecules. The best known representative of this group is heme, the basis of hemoglobin. Porphyrins have an organic structure where in the middle a core exists where metals can bind to the molecule. In figure 1.1a a porphine molecule, which is the simplest porphyrin, can be seen with position numbering. The molecule that is used in this research, called AN153, has functional groups on the meso positions (5, 10, 15 and 20). On the 5 and 15 positions pyridyl groups are added. These groups can bind metals to the nitrogen atoms. On the 10 and 20 positions hexyl chains in trans configuration are added. To distinguish this molecule from a variant where metal binds to the core the non-metallic AN153 will be called 2H-AN153. This molecule can be seen in figure 1.1b.

The project consists of the deposition of Ni-metalized 2H-AN153, which will be called Ni-AN153, on Ag(111). The Ni-AN153 molecule can be seen in figure 1.1c. The deposition of Ni-AN153 will then be investigated using STM. When this sample has been investigated a deposition of cobalt will be done on this sample. The effect of annealing this sample will also be studied. Afterwards the sample will be investigated using X-ray photoelectron spectroscopy, a analysis method using the photoelectric effect to determine the binding energies of specific elements. The results of the analysis will be compared to a previous project done with comparable molecules on the same substrate.

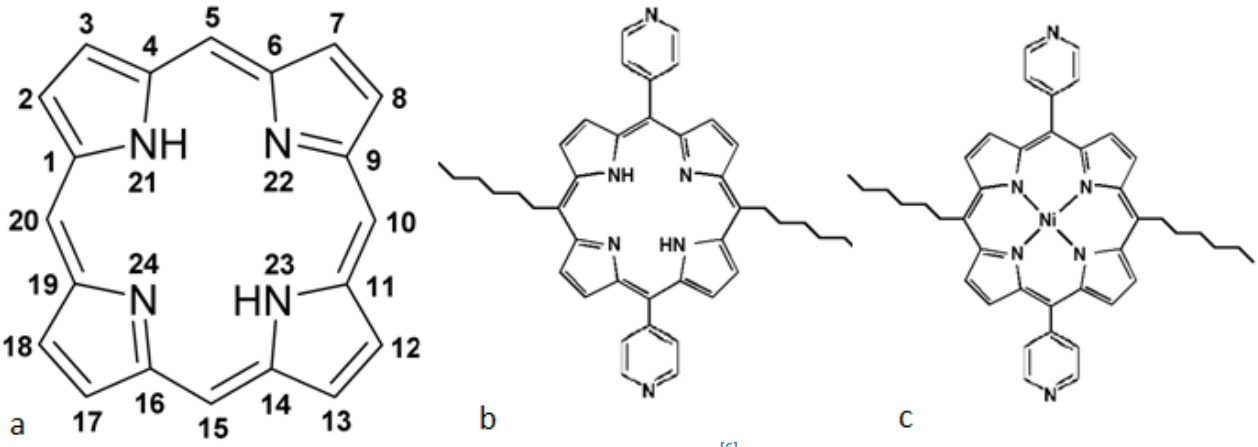

Figure 1.1: a: Porphine, the simplest porphyrin, with position numbering[6]. b: 2H-AN153. c: Ni-AN153.

2) Experimental Techniques

2.1) Environmental factors: temperature and vacuum level

A crucial part of the this research is the environment in which the sample is measured. Two factors are important, temperature and vacuum level. With low temperature it is made sure the particles on the sample, whether it is dust or molecules to be measured, remain static. At room temperature the energy might be high enough for particles to diffuse on the surface. This research is carried out at room temperature.

The other factor one needs to take into account is the vacuum level. At ambient conditions a lot of water and dirt will be present on and around the sample which may interfere with the research. Therefore this research is carried out at ultra high vacuum (UHV). UHV is the vacuum level with pressures between 10^{-9} and 10^{-12} torr[7]. To achieve this vacuum two pumps are used. The first pump is a roughing pump, which takes gas from the system and pushes it through an exhaust valve as demonstrated in figure 2.1. The second pump is a turbo molecular pump, which used a series of angled fast moving rotors to hit particles in the direction of the roughing pump. A schematic picture can be seen in figure 2.2.

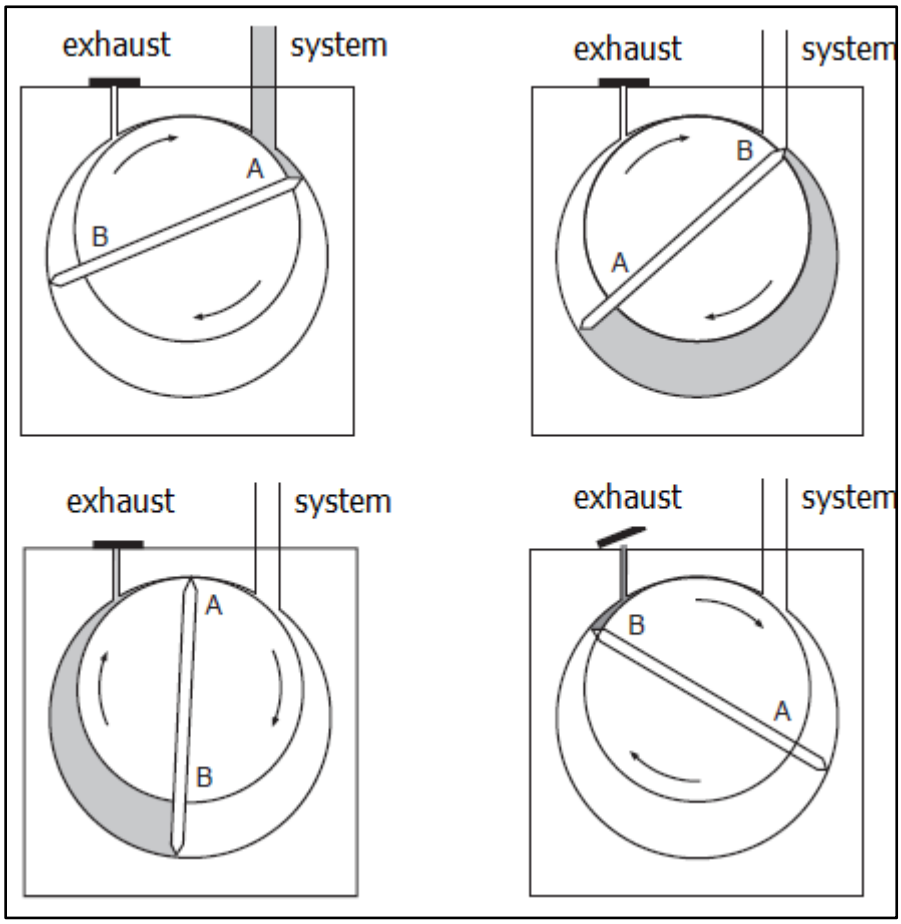

Figure 2.1: The working principle of roughing pump. First gas is taken from the system and then pushed out of the pump[7].

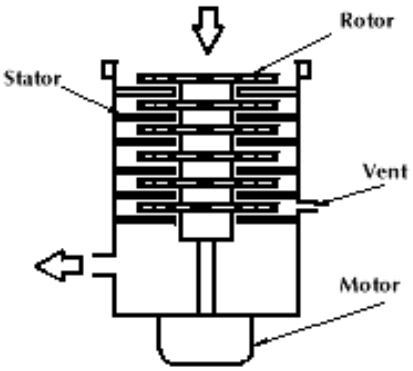

Figure 2.2: A schematic picture of a turbo molecular pump[8]

2.1.1) Bake-out

Before the sample is made the chambers have to be free of water. To achieve this a bake-out is done. The bake-out consists of a bake-out for the evaporators and supplementary parts and a bake-out for the whole system. The evaporators are baked out at 120°C for 24 hours. The system bake-out is also done at 120 °C, but for 48 hours. This way any water in the STM will evaporate.

2.2) Sample preparation

A Ag(111) crystal is used as a sample upon which the Ni-AN153 molecules are deposited. To prepare the sample four steps are taken: First the molecules are degassed, thereafter the silver surface is cleaned and smoothed using cycles of sputtering and annealing. The final step is to deposit the molecules. To deposit the molecules a molecule evaporator is used. The molecules are placed inside a so called Knudsen cell, which can be heated using resistive heating. When the temperature of the evaporator reaches the sublimation temperature of the molecules the molecules will start to sublimate. The gaseous molecules will then adhere to the substrate placed above the heating element. To make sure the outside of the evaporator does not get too hot and the vacuum chambers do not get heated by the evaporator. Water cooling is used in combination with thermal isolation through ceramic shielding. An example blueprint of a molecule evaporator is given in figure 2.3.

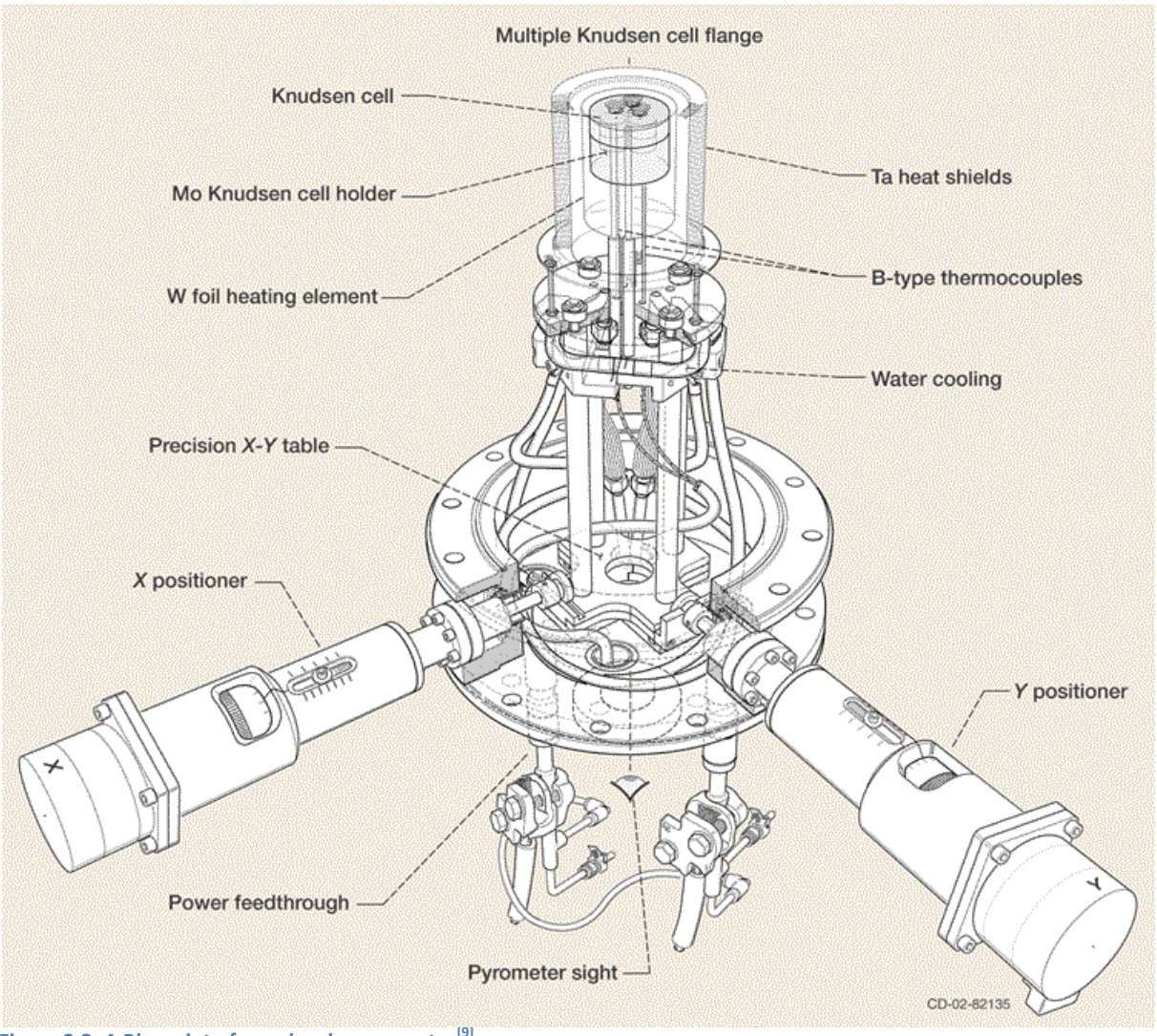

Figure 2.3: A Blueprint of a molecule evaporator[9].

As described in the introduction, part of this research is the investigation of cobalt deposition on the Ni-AN153 network. To deposit cobalt atoms on the sample a metal evaporator is used. This evaporator uses a focused electron beam to evaporate the metal to be deposited. A beam of electrons is focused on metal rods consisting of the evaporant, cobalt. The electrons will hit the evaporant causing it to evaporate and adhere to the sample. As with the molecular evaporator the metal evaporator is water cooled. : A schematic picture of an electron beam evaporator can be seen in figure 2.4.

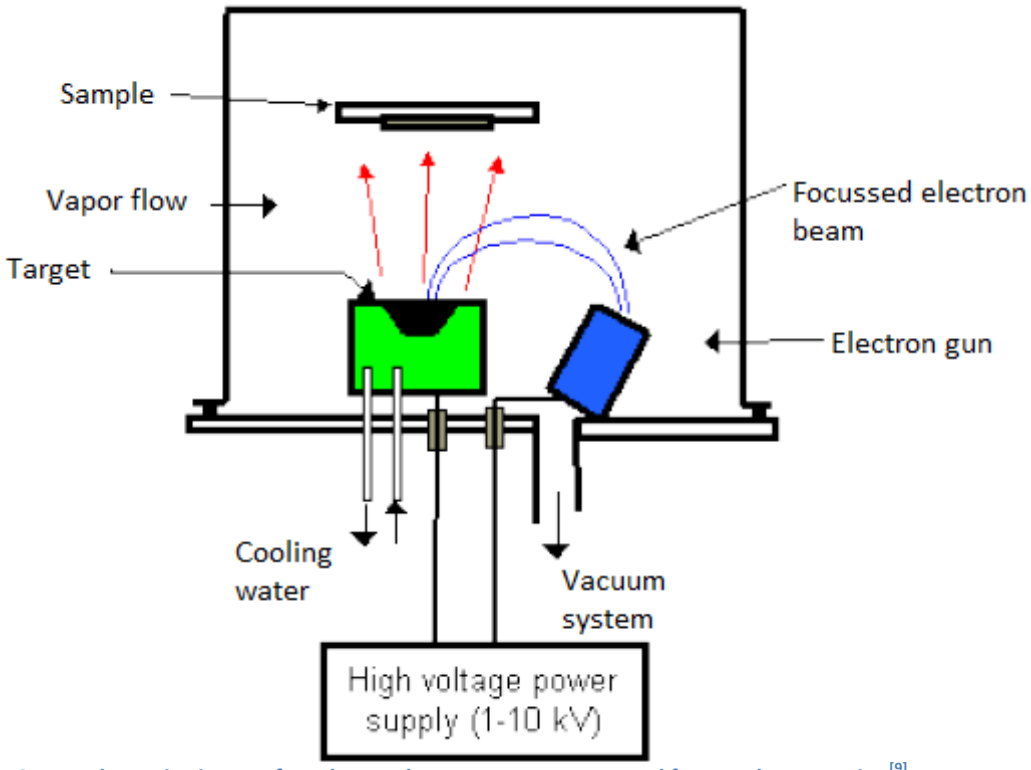

Figure 2.4: A schematic picture of an electron beam evaporator, as used for metal evaporation[9].

2.2.1) Degassing

The next step is to degas the molecules in order to get rid of synthesis impurities. To measure the rate at which the molecules are degassing a quartz crystal microbalance is used. The quartz crystal in the microbalance will oscillate at a frequency that dependents on the thickness of the adsorbate on the crystal. As the rate of evaporation increases the gaseous molecules will attach to the crystal and the frequency will decrease. When the evaporator is degassed the temperature is slowly increased. When the water starts to evaporate a slight change in frequency will be observed. The rate around this point will not be very high, still below 1 Å per minute. At a certain point the molecules in the evaporator will start to sublimate, at this point the rate will rise quickly to beyond 1 Å/min. When this happens the degassing process is stopped and the evaporation temperature of the molecule is noted. For Ni-AN153 the evaporator showed a sublimation at 103°C, however other measurements showed different temperatures ranging up to 280°C. Therefore the 103°C is merely an arbitrary value for the evaporator than a realistic sublimation temperature.

2.2.2) Sputtering and annealing

To clean the silver surface a series of sputtering and annealing is used. Sputtering is a technique where the target, in this case the sample, is bombarded with accelerated Ar^+ ions. When the argon ions hit the surface the top most layers, including any dirt, will be kicked out. As the process also roughens the surface an annealing step is done afterwards.

In the annealing process the sample is heated up to 400°C. When annealing the silver atoms get enough energy to redistribute on the surface and thus a smoother area is created. The atoms displaced by the argon bombardment will have enough energy to redistribute on the surface. Three series of sputtering and annealing where used to prepare the sample to make sure as little dirt as possible was left on the sample.

2.2.3) Molecule deposition

When the sample is entirely clean the molecules will be deposited. To do so the molecule evaporator is again set to the evaporation temperature found during the degassing. The Ni-AN153 is deposited by setting the evaporator to 103°C. Approximately 1 monolayer of molecules, a thickness of 1,2 Å, was deposited for this project. An equivalent to 1 monolayer is favorable, because this will lead to less diffusion, as the molecules will stabilize the network through hydrogen bonds. This is favorable as diffusion hinders a good STM resolution.

2.3) STM

One of the main techniques used to examine the sample is scanning tunneling microscopy (STM). For this invention Gerd Binnig and Heinrich Rohrer were awarded the Nobel Prize in physics in 1986[2][10]. A STM is a non optic microscope based on the quantum principle of tunneling.

2.3.1) Theoretical background

The working principle of the STM is based upon the quantum principle of tunneling. Tunneling occurs when a particle tunnels through a barrier which in classical physics the particle cannot overcome.

This tunneling phenomenon occurs because of evanescent waves in the barrier: when a particle travel through a barrier, the amplitude of the waves, which exist because of the wave-particle duality, will decrease exponentially. There is a probability that the wave travels through the barrier becoming a propagating wave with lower amplitude (see figure 2.5).

A tunneling current will exists when electrons tunnel through oxides or vacuum between two metallic contacts. This tunneling current is exponentially dependent on the distance:

$$I = f(U)e^{-\kappa d} \text{ with } \kappa = 2\sqrt{\frac{m(\phi_1 - \phi_2)}{\hbar}}$$

ħ is the Dirac constant, m is the electron mass, $\phi_{1,2}$ are the work functions of the respective metallic contacts, f(U) is a function describing the electronic structure of the contacts, in a free electron gas this function is approximately the potential (U).

Because of this exponential behavior a small change in distance will lead to a comparable large change in the current. When the STM tip scans over the sample the distance between tip and sample will constantly change. Although this change is very small, in the order of ångströms, they will lead to a notable current change. This principle is used in STM.

When a positive bias is applied, the electrons tunneling to the surface will have an energy of approximately eV, with e the electron charge and V the applied bias. These electrons will interact with the lowest unoccupied molecular orbital (LUMO) of the sample. Within the interval of energy's around eV the local density of states (LDOS) is measured. The topographic image created by the STM is a LDOS contour around the LUMO energy level.[11] This can be calculated to a topographic image of the surface.

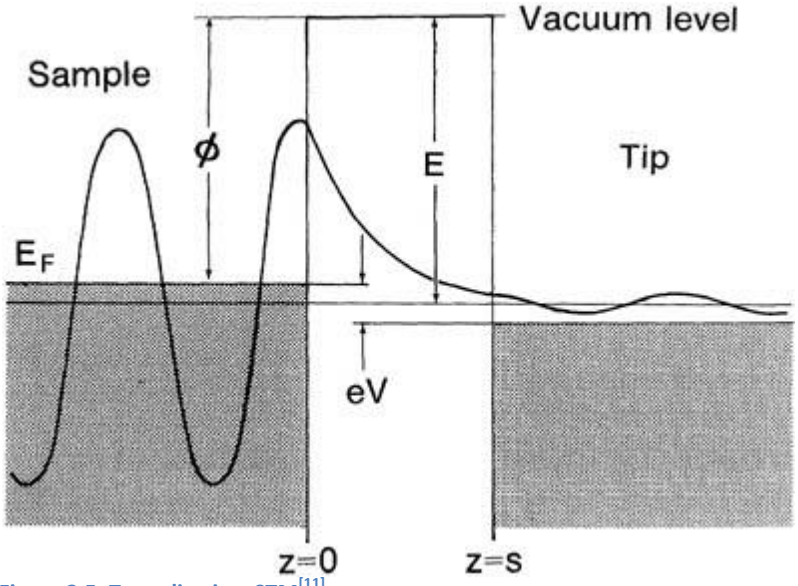

Figure 2.5: Tunneling in a STM[11]

2.3.2) Instrumentation

The main components of a STM are a tip mounted in a piezo tube, a current amplifier and of course a sample to scan (see figure 2.6). Both the tip and the sample have to be of conducting material for tunneling and thus the STM to work.

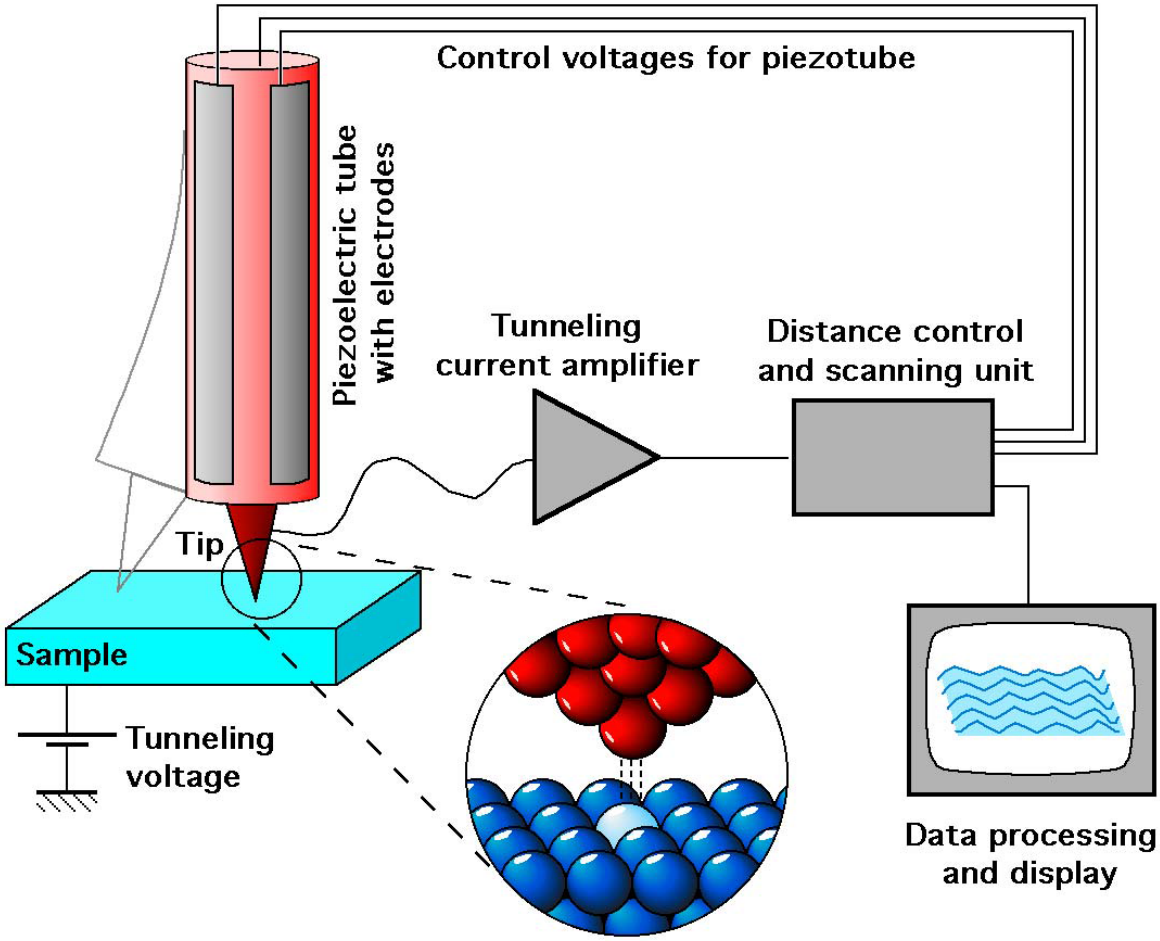

Figure 2.6: A schematic picture of a STM. [12]

Small movements of the tip, in the order of ångströms, are needed to scan the surface. Piezo tubes are used for these movements. Piezo tubes are tubes made of piezoelectric material, which is a material whose stress level is dependent on the accumulated charge. Currently, most piezo tubes are divided in 4 segments, when a current is applied to one of these segments it will expand or contract. When one of these 4 segments contracts the tip will move to that direction, and if it expands it will push the tip to the opposite direction, thus allowing movement in the +x, -x, +y and –y directions. To approach the tip to the sample another piezo element is used to allow movement in the z-direction by expanding or contracting.

The tip is usually made from either tungsten (W) or an alloy of platinum (Pt) and iridium (Ir). The W tip is made using chemical etching, this is done by putting part of a W wire in a NaOH or KOH solution and applying a bias between the W wire and a counter electrode. The disadvantage of this tip is that in ambient conditions the tip will oxidize. As oxides do not conduct the tip is no longer conductive, so it cannot be used for STM. Therefore the tip has to be used under ultra high vacuum, as it will not oxidize under these conditions. The other kind of tip, the Pt/Ir alloy, is made by taking a Pt/Ir wire and cutting it diagonally using a wire cutter. The advantage of this tip is that is it much easier to prepare and can be used under all conditions, including vacuum, low temperature and ambient conditions. The difference between these tips can be seen in figure 2.7.

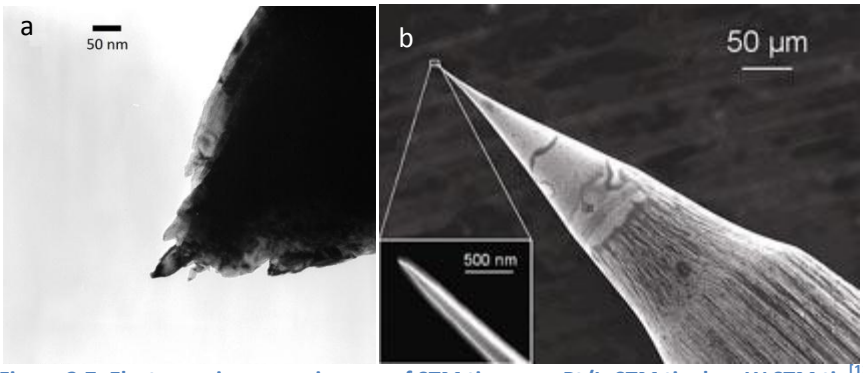

Figure 2.7: Electron microscopy images of STM tips. a: a Pt/Ir STM tip. b: a W STM tip[13].

The tunneling current between tip and sample will always tunnel from the point of the tip that is closest to the sample. Therefore the atom on the tip which is closest to the sample will admit 99% of the tunneling current. The rest of the atoms on the tip do hardly contribute to the tunneling process Therefore the only thing that matters when looking at a STM tip is that it is atomically sharp. There are only two ways in which a tip can hinder the imaging process. One way is if two atoms are both at the closest distance to the sample, this way a double topographic picture will be constructed.

Another way the scanning process can be hindered is when the tip picks up material from the sample, because molecule might diffuse onto the tip during the scanning process. This material can lead to a disruption of the measurement of the distance between sample and tip. To drop these materials from the tip pulses ranging up to 10V are used. By the sudden increase in bias over a short time the material might drop from the tip. The tip may also pick up more material when this pulse is used. This is a matter of patience until the tip lets go off the material. To make sure the tip is clean a cupper surface can also be used. As there are no molecules on the sample the tip cannot pick any molecular material up and can only be improved.

2.3.3) STM measurement modes

There are two STM operating modes. One mode is the constant current mode, in which the current is kept constant and the tip adjusts to the height of the sample.. By recording the z position of the tip while scanning the sample a topographic image is constructed. The other mode is the constant height mode, in which the height is kept constant, but the change in current, due to the changing distance between sample and tip, is measured. Through this change in current the topographic image is constructed. Typical tunneling currents range from 0.01 till 50 nA[7]. This current is transformed in a voltage using a current amplifier. This voltage is fed into the z-directional piezo elements as a feedback voltage to keep the current or position constant. In this research only the constant current mode was used.

2.3.4) Vibration isolation

To keep external vibrations from interfering with the STM, the microscope is mounted on a stage which is damped using eddy currents. An eddy current is a current induced in a conductor by a changing magnetic field. On the edge of the stage copper blocks are mounted, under these blocks magnets are placed. When the copper blocks move towards the magnets a current is induced in the copper blocks. This current will lead to a force to counteract the movement towards the magnets causing the stage to float on the magnets (see figure 2.8). When any external movements interfere with the stage this magnetic force, along with gravity, will bring the stage back to the equilibrium position.

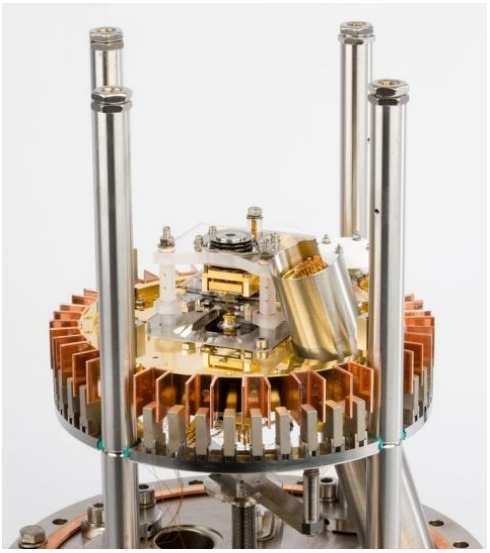

Figure 2.8: A STM stage using eddy current damping[14]

2.4) XPS

X-ray photoelectron spectroscopy (XPS), also known as electron spectroscopy for chemical analysis (ESCA)[15] is a surface analysis technique based on the photoelectric effect[7]. When X-rays are shot at the sample electrons close to the core of the atom will be kicked out of their orbit. The XPS measures the kinetic energy and number of electrons emitted from the sample. With this information two things can be determined. Firstly, the energy of the electrons is dependent on the chemical surroundings of the element, a slight shift might give information on the state of the material. Secondly, the energy of the core electron is unique for each element. Therefore the electron intensity at certain energy levels can be used to determine which elements and how much of these elements are present on the surface. A schematic representation of XPS is shown in figure 2.9.

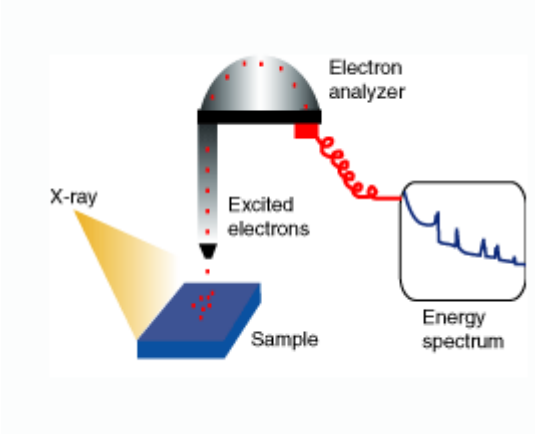

Figure 2.9: Schematic representation of XPS[16].

3) Results

3.1) STM data of Ni-AN153 on Ag(111)

Approximately 1,2 Å of Ni-AN153 was deposited on Ag(111), which is equivalent to one monolayer. The molecules self-assemble in a close packed network. In figure 3.1 an overview of the structure after deposition of Ni-AN153 on Ag(111) is shown.

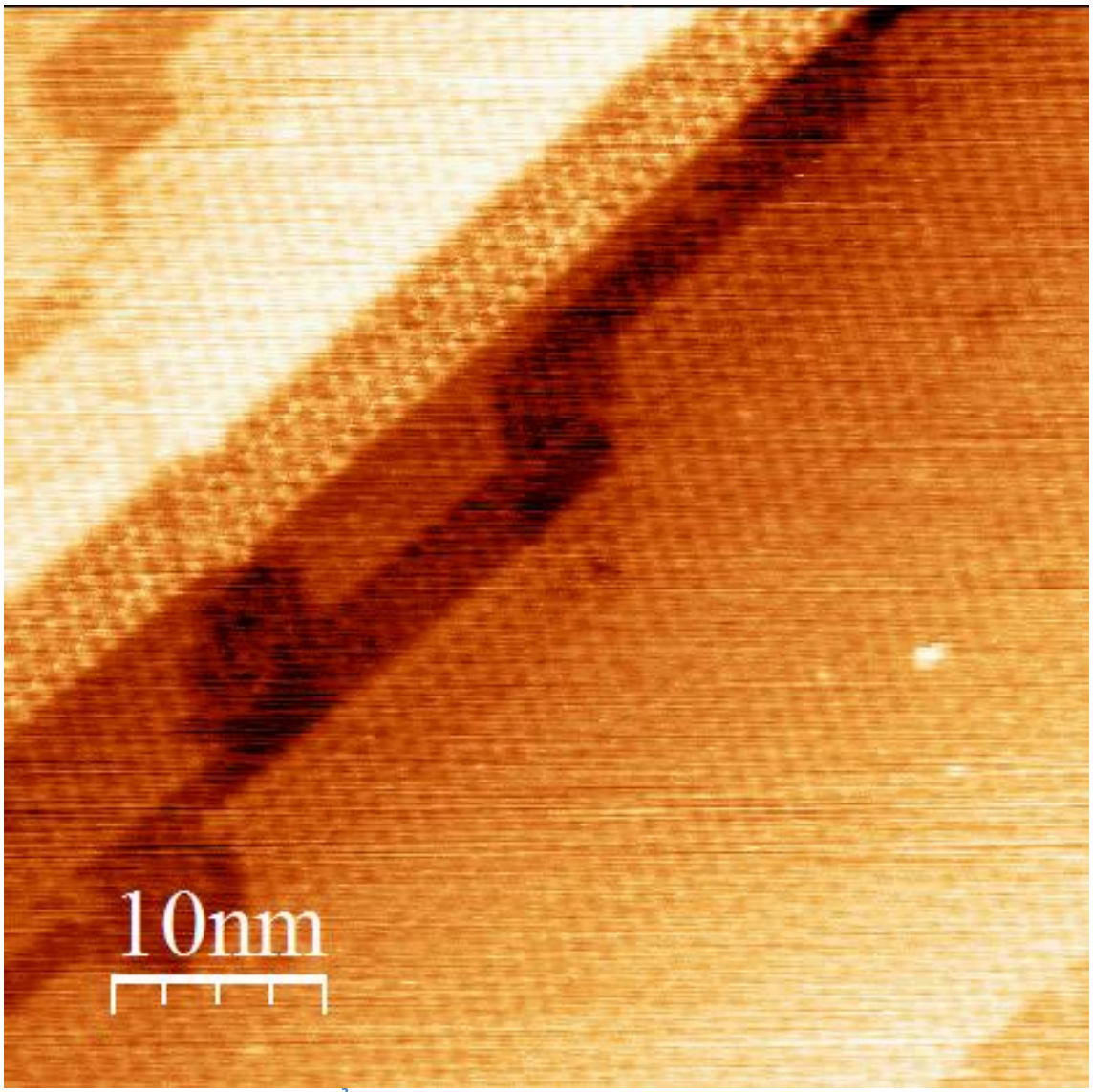

Figure 3.1: A STM image (50x50 nm^2, -1.8 V, 25 pA)of the self-assembly of Ni-AN153 on Ag(111). The covarage was approximately 1 monolayer. The observed phase is a close packed network.

In order to obtain any information on the lattice, the parameters of the unit cell, as shown in figure 3.3, have to be determined. To determine the parameters of this close packed structure, an analysis of the STM image is done using the program WSxM 5.0 Develop 6.3[17]. First a zoom of the structure is made. After this the lattice can be seen as demonstrated in figure 3.2, a Ni-AN153 molecule is also added in the figure for size comparison. To determine the lattice parameters of the unit cell the height profiles along line A and B are used. In figure 3.2 the lines can be seen along which the height profile was determined.

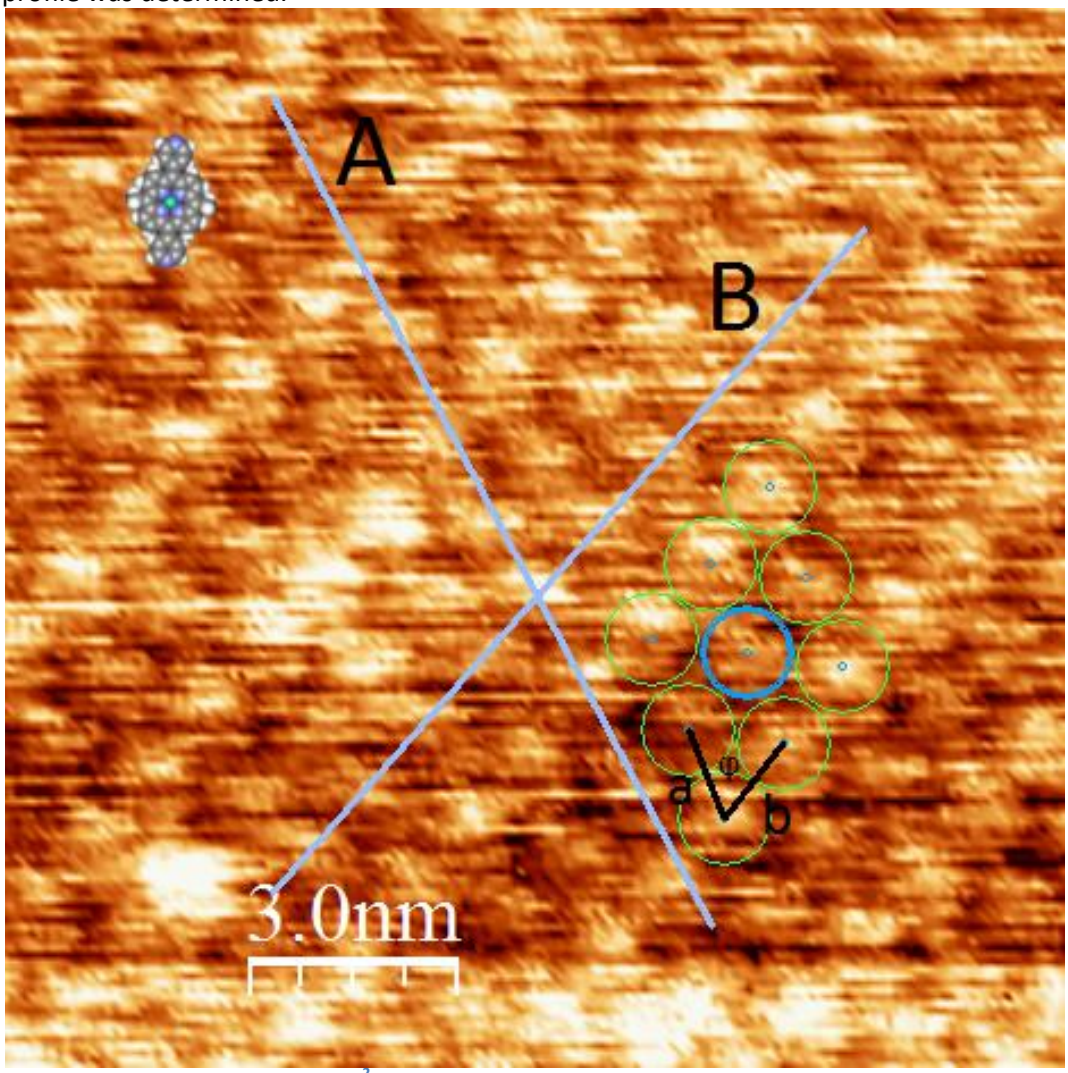

Figure 3.2: A STM image (15x15 nm^2, -1.8 V, 25 pA) of the close packed network of Ni-AN153 on Ag(111). The covarage was approximately 1 monolayer. On the STM image the lattice of the close packed network is shown with green and blue circles. Each circle represents one Ni-AN153 molecule. In this network the unit cell parameters are shown. The lines along which a height profile of the close packed network was determined, in order to determine the unit cell parameters, are shown as line A and B. On the top left a Ni-AN153 molecule can be seen for size comparison.

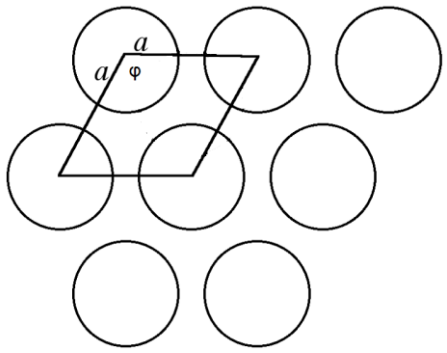

Figure 3.3: Unit cell for the close packed network.

The following height profiles where found:

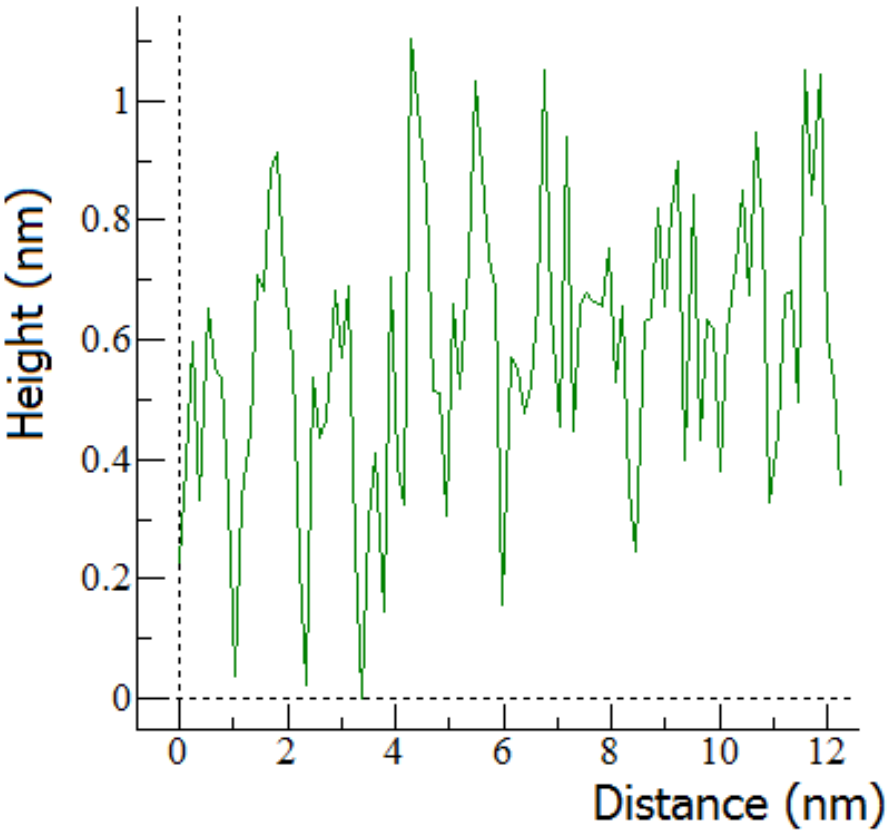

Graph 3.1: The height profile along line A as drawn in figure 3.2.

In graph 3.1 the height profile of line A can be seen. 10 Peaks are observed, coinciding with the 10 molecules that are along line A, which can be seen as bright spots in figure 3.2. The distance from first to last peak, 9 times the distance between molecules, equals 11.26 nm. This corresponds to a distance of 1.25 nm between molecules.

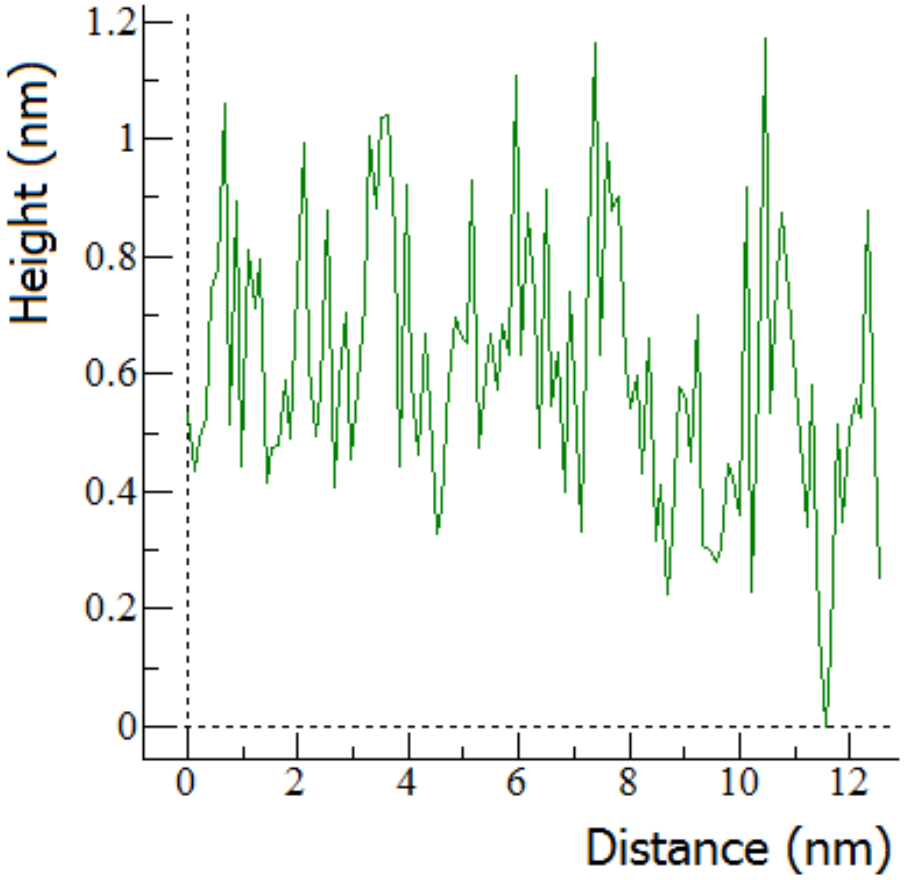

Graph 3.2: The height profile along line B as drawn in figure 3.2.

In graph 3.2 the height profile of line B can be seen. 9 Peaks are observed, coinciding with the 9 molecules that are along line B, which can be seen as bright spots in figure 3.2. The distance from first to last peak, 8 times the distance between molecules, equals 11.69 nm. This corresponds to a distance of 1.46 nm between the molecules.

By averaging the distances found along lines A and B, for this STM image and an additional STM image, the following unit cell parameters where found:

a=b=1.35 nm
ϕ=60°

Table 3.1: Unit cell parameters for the close packed network found for Ni-AN153 on Ag(111).

3.2) STM data of Ni-AN153 on Ag(111) after cobalt deposition

After the investigation of 1 monolayer of Ni-AN153 on Ag(111), 0.05 Å of cobalt was deposited. At first the cobalt did not seem to mix with Ni-AN153. The cobalt appeared in islands on the surface. Along with these cobalt islands, two structures where observed on the sample: a close packed network similar to the one observed before and a hexagonal phase, which showed 3 fold symmetry. In figure 3.4 a STM image of the close packed network similar to the previous network is shown At the left of the molecules the islands of cobalt can be seen.

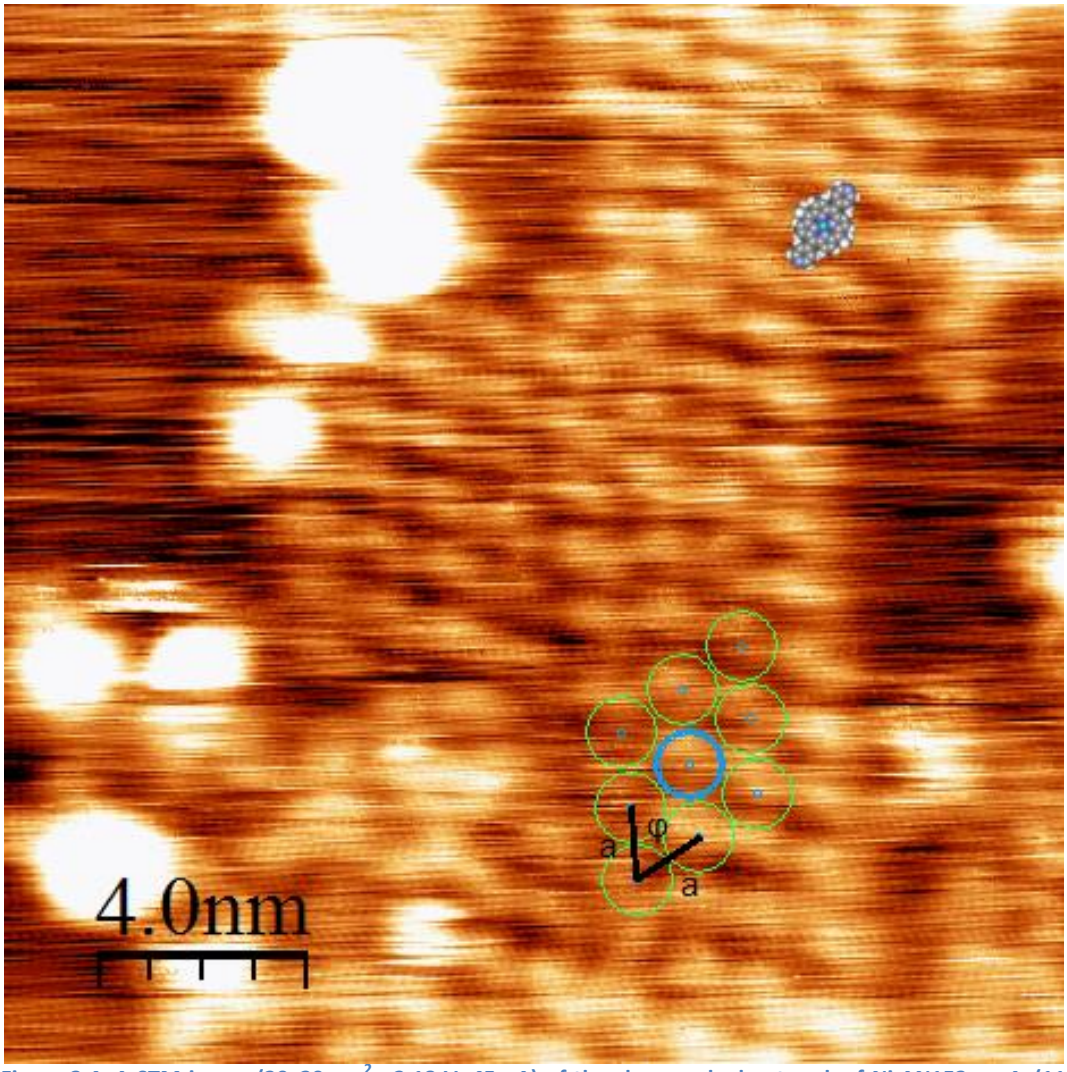

Figure 3.4: A STM image (20x20 nm^2, -2.18 V, 45 pA) of the close packed network of Ni-AN153 on Ag(111) after cobalt deposition. The covarage was approximately 1 monolayer. On the STM image the lattice of the close packed network is shown with green and blue circles. In the network the unit cell parameters are shown. Each circle represents one Ni-AN153 molecule. At the left of the picture islands of cobalt can be seen as bright white dots. On the top right a Ni-AN153 molecule can be seen for size comparison.

The lattice parameters where determined in the same way as shown in the previous chapter, by measuring the height profile and determining the distance between molecules. The following unit cell parameters where found

a=1.39 nm
ϕ=60°

Table 3.2: Unit cell parameters for the close packed network found for Ni-AN153+Co on Ag(111).

The value of a is almost equal to the one found in the close packed network of Ni-AN153 without cobalt, and it can be assumed that these phases are in fact the same. This would mean that the cobalt did not bind to the Ni-AN153 molecule.

The second network that was found was a 3-fold symmetric hexagonal network. As this is no longer a close packed structure, the new unit cell parameters need to be determined. A STM image of the network is shoen in figure 3.5 and the new parameters are shown in figure 3.6.

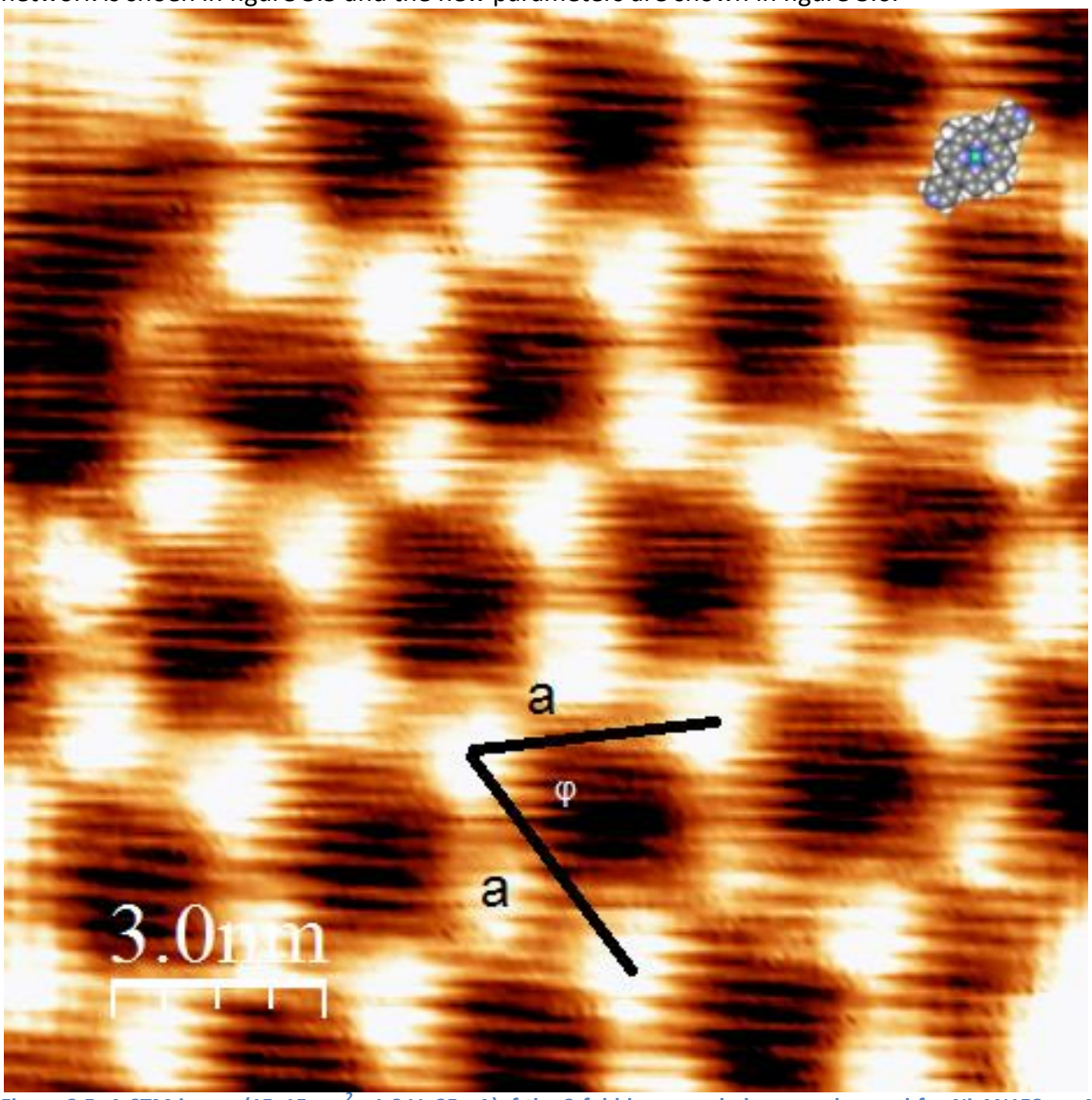

Figure 3.5: A STM image (15x15 nm^2, -1.8 V, 25 pA)of the 3-fold hexagonal phase as observed for Ni-AN153 on Ag(111) after cobalt deposition. The covarage was approximately 1 monolayer. In the image the unit cell parameters are shown. On the top right a Ni-AN153 molecule can be seen for size comparison.

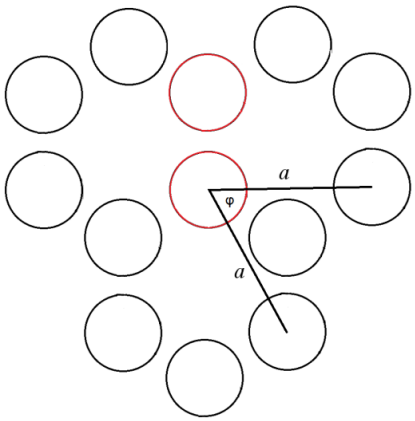

The unit cell parameters as marked in figure 3.6 where found to be:

a=3.28 nm
ϕ=60°

Table 3.3: : Unit cell parameters for the hexagonal network formed by Ni-AN153+Co on Ag(111).

Figure 3.6: 3-fold hexagonal network with repetitive structure shown in red and unit cell parameters indicated.

To give the sample enough energy for the cobalt atoms and the Ni-AN153 molecules to mix the sample is annealed. This is done at 200°C for 20 minutes. After the annealing two phases where observed. The initial close packed network seen before annealing was still present and in addition a new phase was observed. The close packed network similar to the initial network is shown in figure 3.7. For this network the following unit cell parameters where found:

a=1.49 nm
ϕ=60°

Table 3.4: Unit cell parameters for the hexagonal network found for Ni-AN153+Co on Ag(111) after annealing.

This value is again close to the initial value of Ni-AN153 without cobalt and the value for Ni-AN153 with cobalt before annealing, therefore it is assumed that the cobalt did not bind to the AN153 in this phase. The values increase slightly compared to the previous found values as the annealing excites the molecular bonds, causing them to expand.

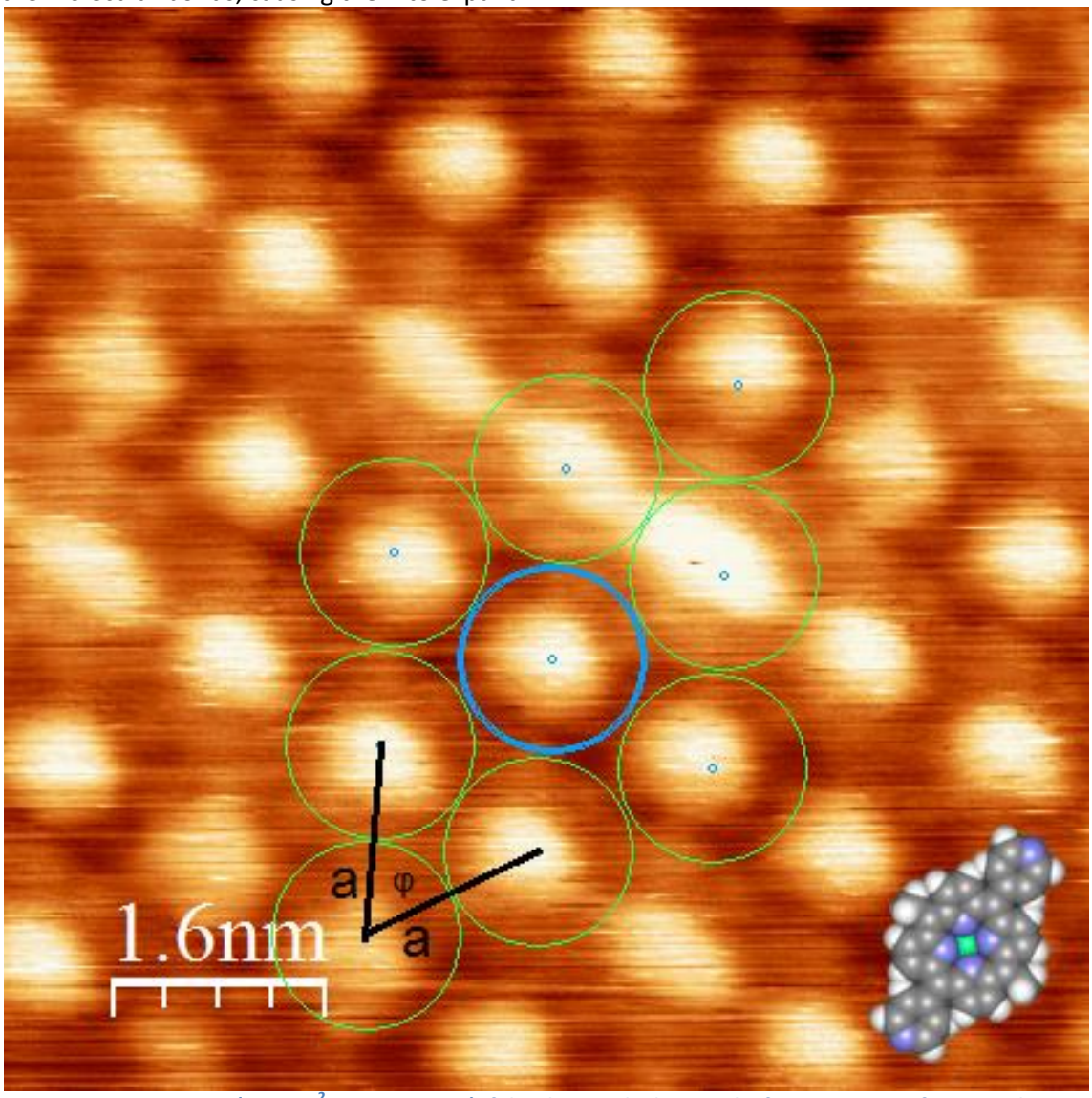

Figure 3.7: A STM image (8x8 nm^2, -1.24 V, 35 pA)of the close packed network of Ni-AN153+Co after annealing on Ag(111). The covarage was approximately 1 monolayer. In the STM image the lattice of the close packed network is shown with green and blue circles. In the network the unit cell parameters are shown. Each circle represents one Ni-AN153 molecule. On the bottom right a Ni-AN153 molecule can be seen for size comparison.

The new phase that was found after the annealing of the sample is shown in figure 3.8. A repetitive pattern can be seen of which the unit cell parameters will be determined along line A and B as indicated.

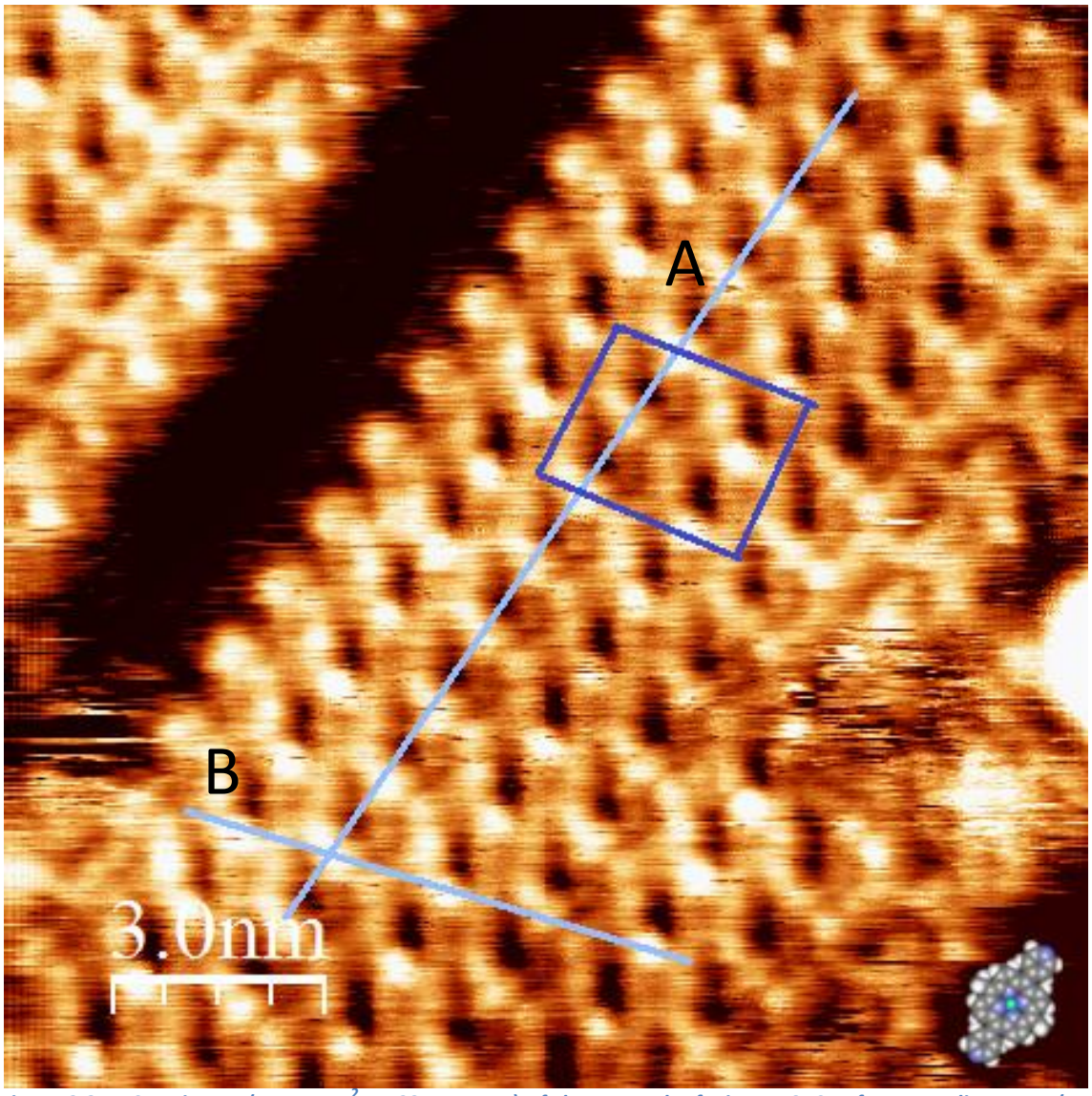

Figure 3.8: A STM image (15x15 nm^2, -1.23 V, 75 pA) of the network of Ni-AN153+Co after annealing on Ag(111). The covarage was approximately 1 monolayer. A repetitive structure can be seen. The blue parallelogram marks the unit cell. The lines along which the unit cell parameters are determined are also shown. On the bottom right a Ni-AN153 molecule can be seen for size comparison.

The following height profiles where found:

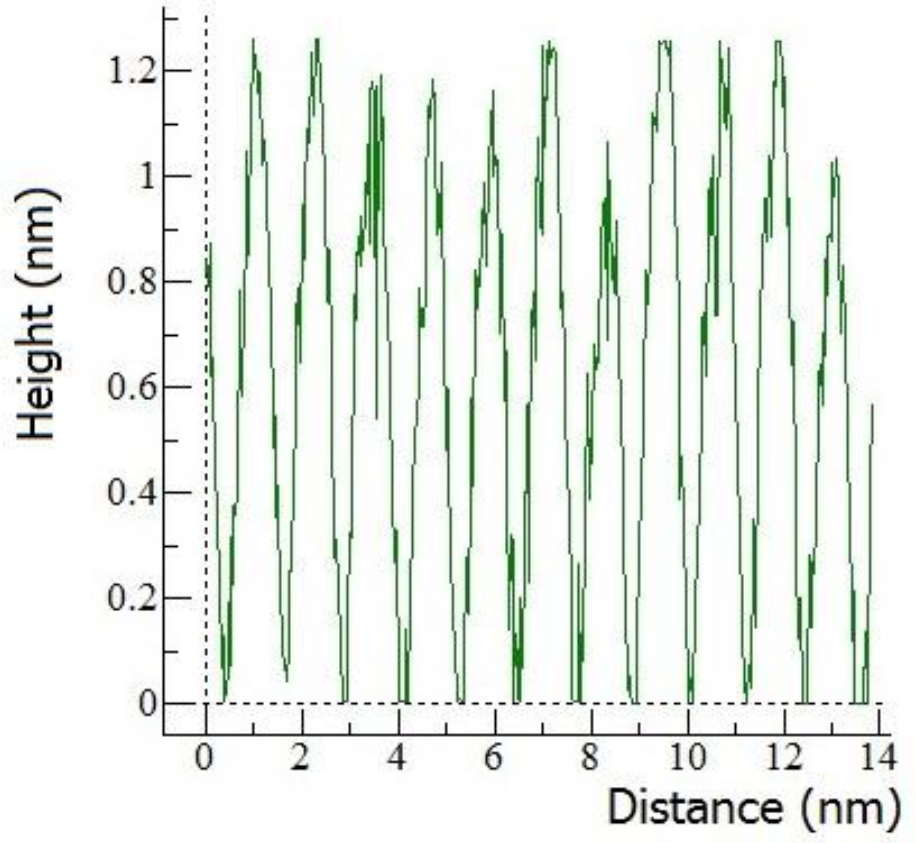

Graph 3.3: The height profile of line A as shown in figure 3.8.

In graph 3.3 the height profile along line A can be seen. 11 Peaks are observed, coinciding with the 11 molecules that are on line A, which can be seen as bright spots in figure 3.8. The distance from first to last peak, 10 times the distance between molecules, equals 11.98 nm. This corresponds to a distance of 1.20 nm between molecules.

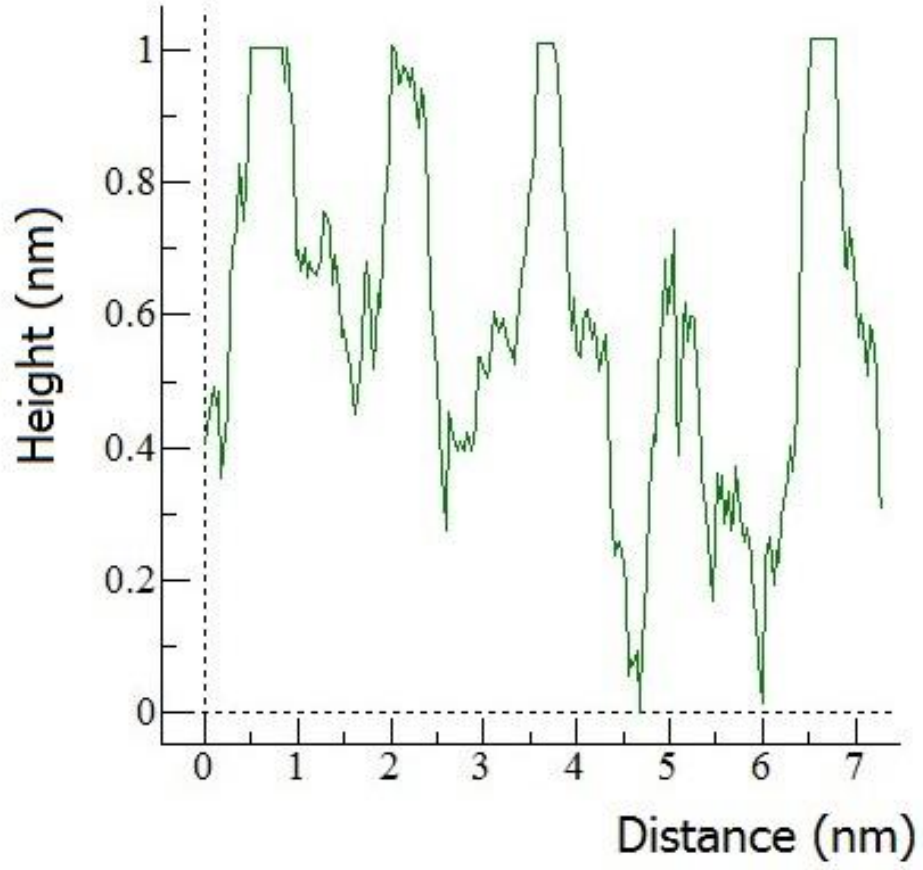

Graph 3.4: The height profile from line B as shown in figure 3.8.

In graph 3.4 the height profile along line B can be seen. 5 Peaks are observed, coinciding with the 5 molecules that are on line B, which can be seen as bright spots in figure 3.8. The distance from first to last peak, 4 times the distance between molecules, equals 5.98 nm. This corresponds to a distance of 1.49 nm between molecules.

3.3) XPS data of nickel in Ni-AN153+Co on Ag(111)

The last step is an XPS analysis of the sample. This is done as the last step, because the X-rays can damage the sample, making it unusable for STM afterwards. Both nickel and cobalt were investigated in between two silver investigations. For example nickel was measure by doing a XPS analysis of silver, than of nickel and then again of silver. This way the silver values can be used to determine the present noise shift. For the silver the energy of the peaks of the 3d orbital are measures, two peaks are observed because of the spin-orbit coupling in this orbital. Two nickel measurements are done, one before the annealing and one after the annealing. For nickel the $2p_{3/2}$ peak energy was measured. In graph 3.5 and 3.6 the silver measurements before and after the nickel measurement before annealing can be seen.

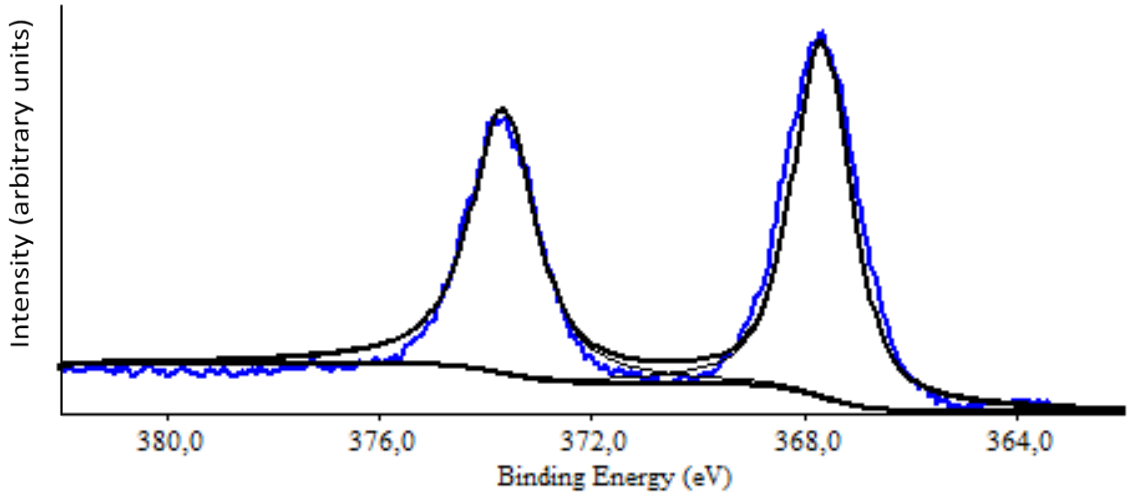

Graph 3.5: The silver 3d XPS spectrum as measured before the measurement of nickel in Ni-AN153+Co on Ag(111).

The silver 3d peaks before the nickel measurement, as shown in graph 3.5, are located at 373.7 eV and 367.7 eV. Compared to the literature values[18] of metallic silver, 374.3 eV and 368.3 eV, this is a chemical shift of -0.6 eV.

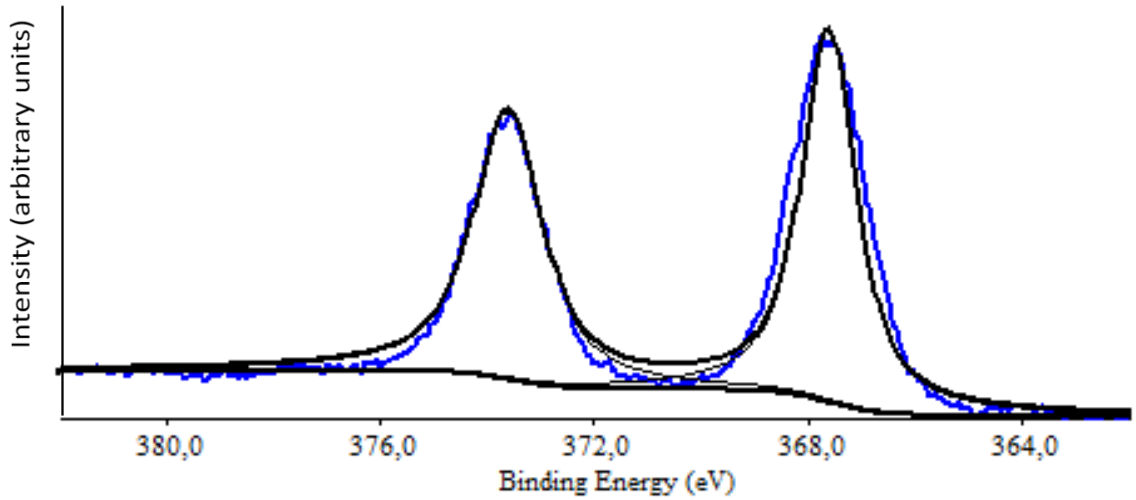

Graph 3.6: The silver 3d XPS spectrum as mesured after the measurement of nickel in Ni-AN153+Co on Ag(111).

The silver 3d peaks after the nickel measurement, as shown in graph 3.6, where found at 373,6 eV and 367.6 eV. Compared to the literature values[18] of metallic silver of 374.3 eV and 368.3 eV this is a chemical shift of -0.7 eV.

The correction of the nickel measurement before annealing averages to -0.7 eV.

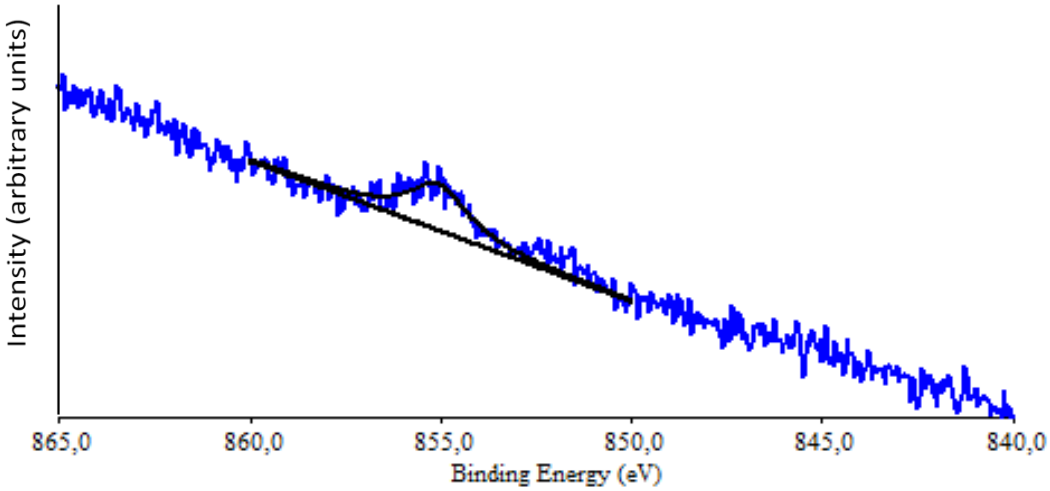

Graph 3.7: The XPS spectrum of nickel $2p_{3/2}$ in Ni-AN153+Co on Ag(111) before annealing.

In graph 3.7 the nickel $2p_{3/2}$ XPS spectrum before annealing can be seen. The observed peak is situated at 855.1 eV. Compared to the literature value[18] of metallic nickel, 852.7 eV, this is a chemical shift of 2.4 eV. When the correction of -0.7 eV based on the silver results is done, the peak will appear at a chemical shift of 1.7 eV.

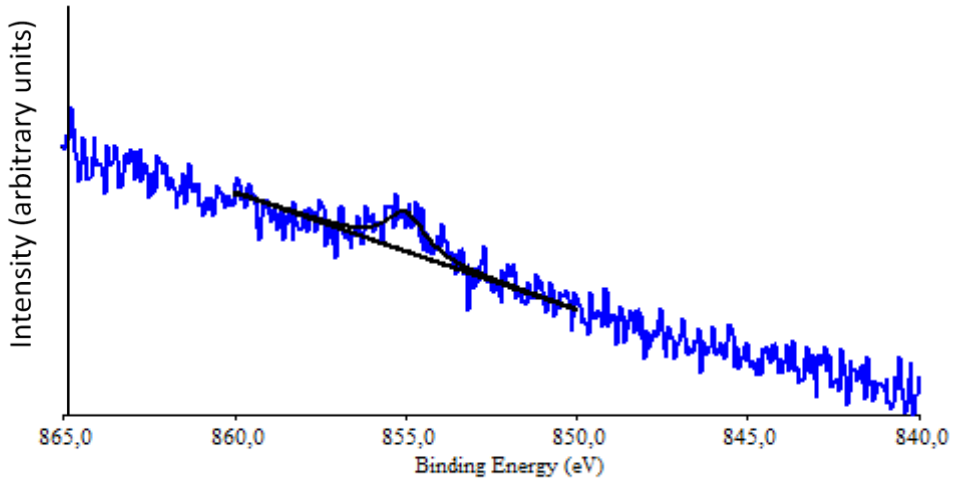

Graph 3.8: The XPS spectrum of nickel $2p_{3/2}$ in Ni-AN153+Co on Ag(111) after annealing.

In graph 3.8 the nickel $2p_{3/2}$ XPS spectrum after annealing can be seen. The observed peak is situated at 855.0 eV, compared to the literature value[18] of metallic nickel, 852.7 eV, this is a chemical shift of 2.3 eV. Using the same method as demonstrated before the correction based on the silver results was -0.7 eV. With this correction the peak appears at a chemical shift of 1.6 eV.

3.4) XPS data of cobalt in Ni-AN153+Co on Ag(111)

Two cobalt XPS measurements of the Ni-AN153+Co sample were done to compare the results before and after annealing. For cobalt the $2p_{3/2}$ peak energy was measured.

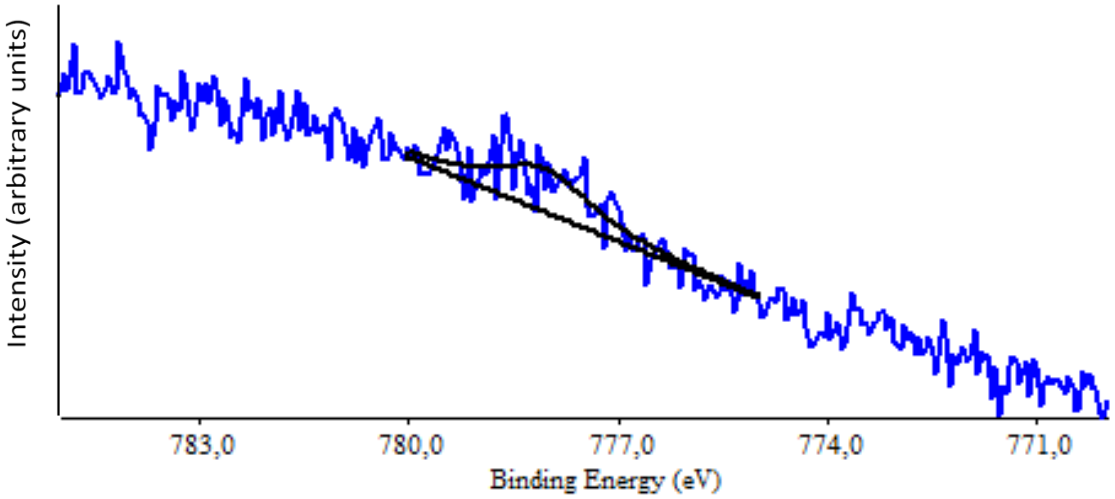

Graph 3.9: The XPS spectrum of cobalt $2p_{3/2}$ in Ni-AN153+Co on Ag(111) before annealing.

In graph 3.9 the XPs spectrum of cobalt $2p_{3/2}$ before annealing can be seen. The observed peak is situated at 778.1 eV, compared to the literature value[18] of metallic cobalt, 778.3 eV, this is a chemical shift of 0.4 eV. Using the same method as demonstrated before the correction based on the silver results was -0.6 eV. With this correction the peak appears at a chemical shift of -0.2 eV.

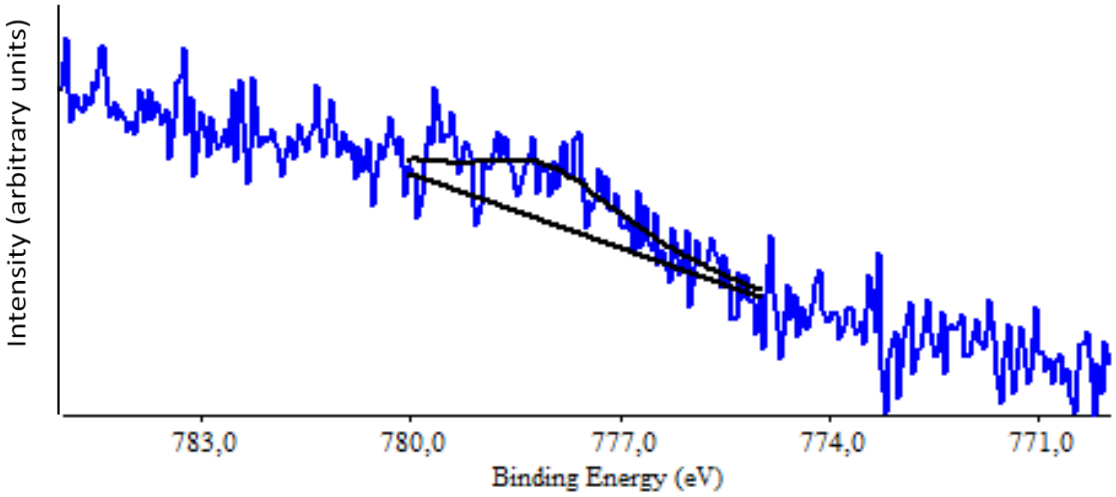

Graph 3.10: The XPS spectrum of cobalt $2p_{3/2}$ in Ni-AN153+Co on Ag(111) after annealing.

In graph 3.10 the XPs spectrum of cobalt $2p_{3/2}$ after annealing can be seen. The observed peak is situated at 778.1 eV, compared to the literature value[18] of metallic cobalt, 778.3 eV, this is a chemical shift of 0.2 eV. Using the same method as demonstrated before the correction based on the silver results was -0.7 eV. With this correction the peak appears at a chemical shift of -0.5 eV.

4) Discussion

4.1) Comparable STM study

In a comparable study 2H-AN153 was deposited on Ag(111). Afterwards cobalt was added to the sample and the sample was annealed.

The self-assembly of 2H-AN153 on Ag(111) was investigated using STM. The resulting STM image can be seen in figure 4.1. This image is used to determine the network of the self-assembly and the distance between molecules. The network observed when 2H-AN153 is deposited on Ag(111) is a close packed network with the following parameters:

a=1.24 nm
ϕ=90°

Table 4.1: Parameters for the close packed network of 2H-AN153 on Ag(111).

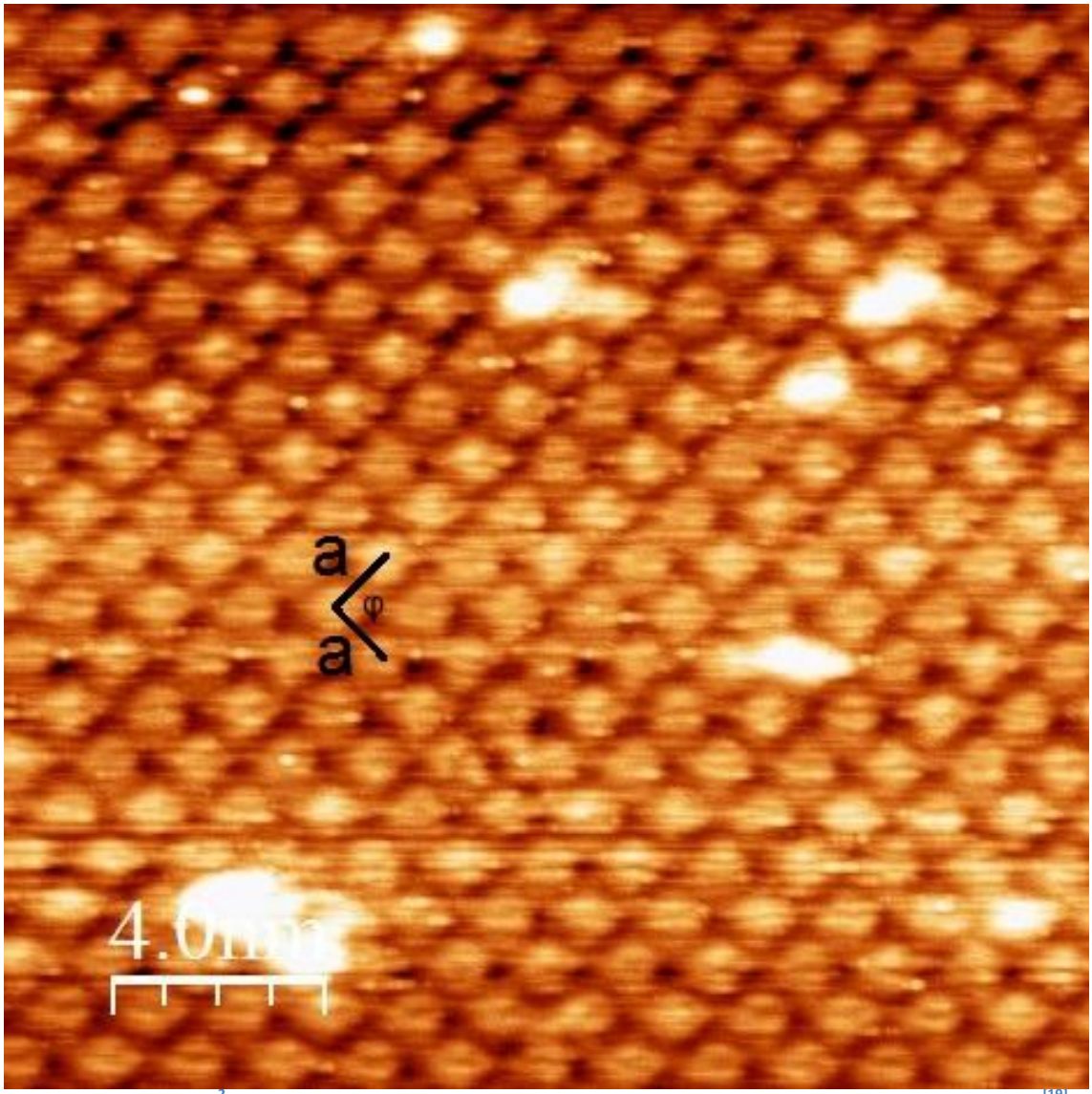

Figure 4.1: A 20x20 nm^2 STM image of the square network observed when 2H-AN153 is deposited on Ag(111)[19].

The second step was the deposition of cobalt on the sample. After the cobalt deposition a new phase was formed, a 3-fold hexagonal stucture. A STM pictue of this phase can be seem in figure 4.2. The following parameters were found for this structure:

a=3.04 nm
ϕ=60°

Table 4.2: Parameters for the 3-fold hexagonal network of 2H-AN153 on Ag(111) after cobalt deposition.

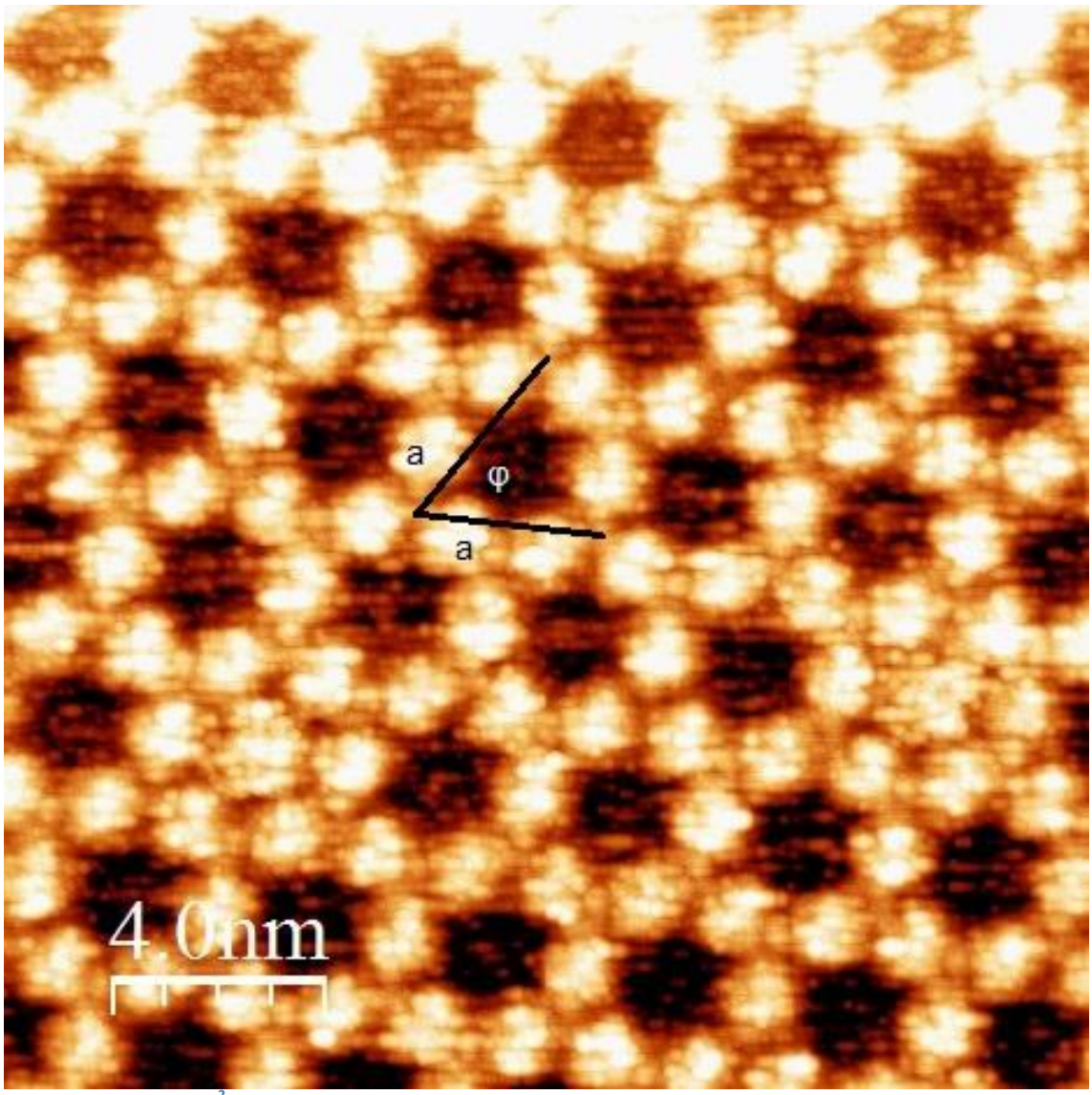

Figure 4.2: A 20x20 nm^2 STM image of the 3-fold hexagonal network of 2H-AN153 on Ag(111) after cobalt deposition[19].

To give the sample enough energy for the cobalt atoms and the Ni-AN153 molecules to mix the sample is annealed. This changed the network back into close packed structure. A STM pictue of this phase can be seem in figure 4.3. The parameters of this network were:

a=1.43 nm
ϕ=60°

Table 4.3: Parameters for the 3-fold hexagonal network of 2H-AN153 on Ag(111) after cobalt deposition and annealing at 200°C.

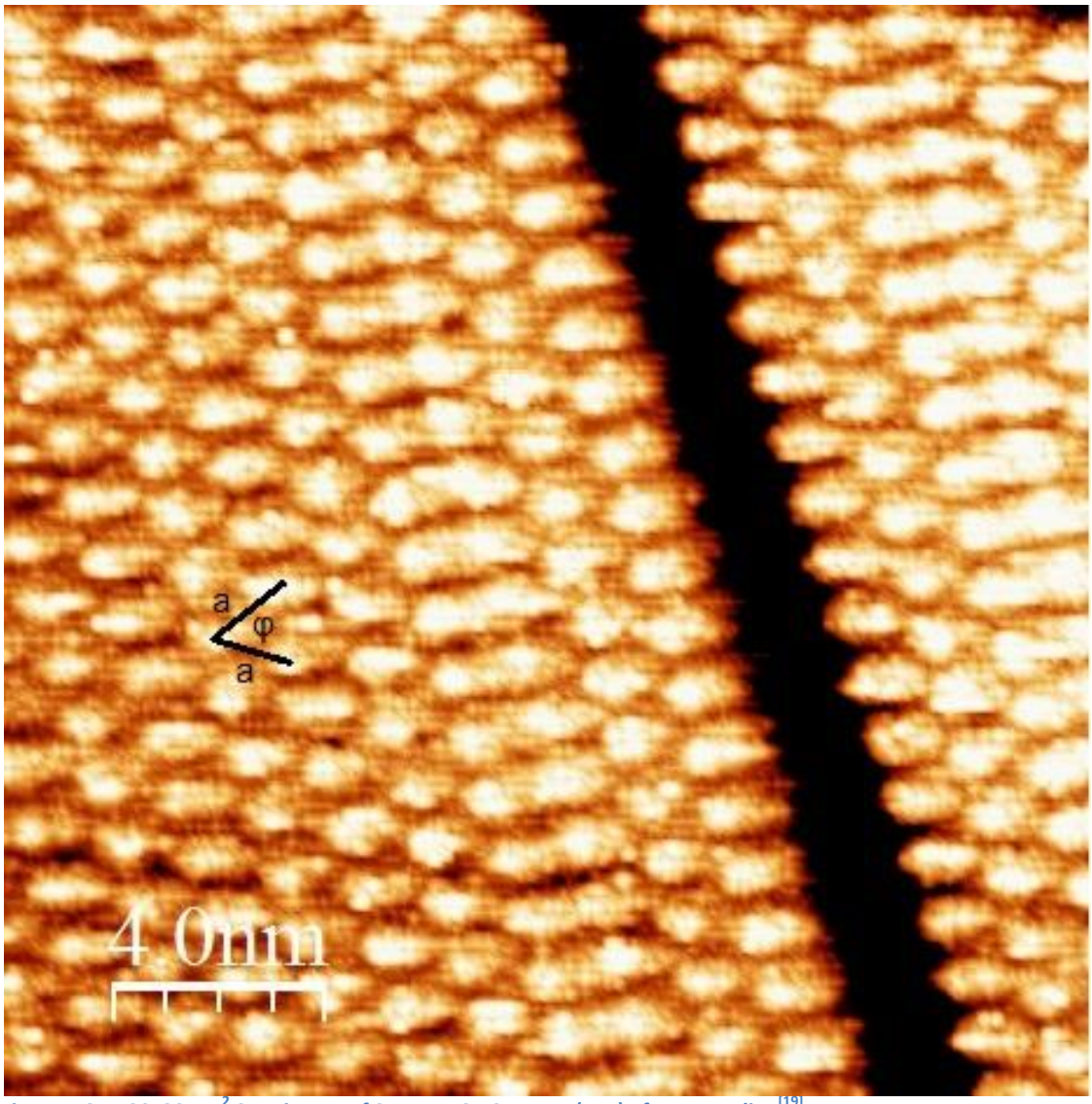

Figure 4.3: A 20x20 nm^2 STM image of 2H-AN153 +Co on Ag(111) after annealing[19].

4.2) Binding motifs of the porphyrin assemblies

To place the molecules onto the STM images Adobe Photoshop 7.0 was used. The first phase that was found, the network of Ni-AN153 without cobalt (figure 3.3, 3.4 and 3.7), is a close packed network, as well as the networks of 2H-AN153 and 2H-AN153 with cobalt after annealing. It is assumed these networks exist because of hydrogen bonds between the nitrogen of the pyridyl groups and the hydrogen of the porphine. A model of this phase superimposed on the STM image shown in figure 3.8 is shown in figure 4.4. It is thought that the when the molecule assembles into this structure the hexyl chains will point up from the surface. It can be assumed that due to the rising of these chains the molecules can pack closer together, causing in an decrease in the energy needed for this structure. This energy decrease will have to overcome the energy increase that is needed to lift these chains up. In figure 4.4 these chains are therefore not shown.

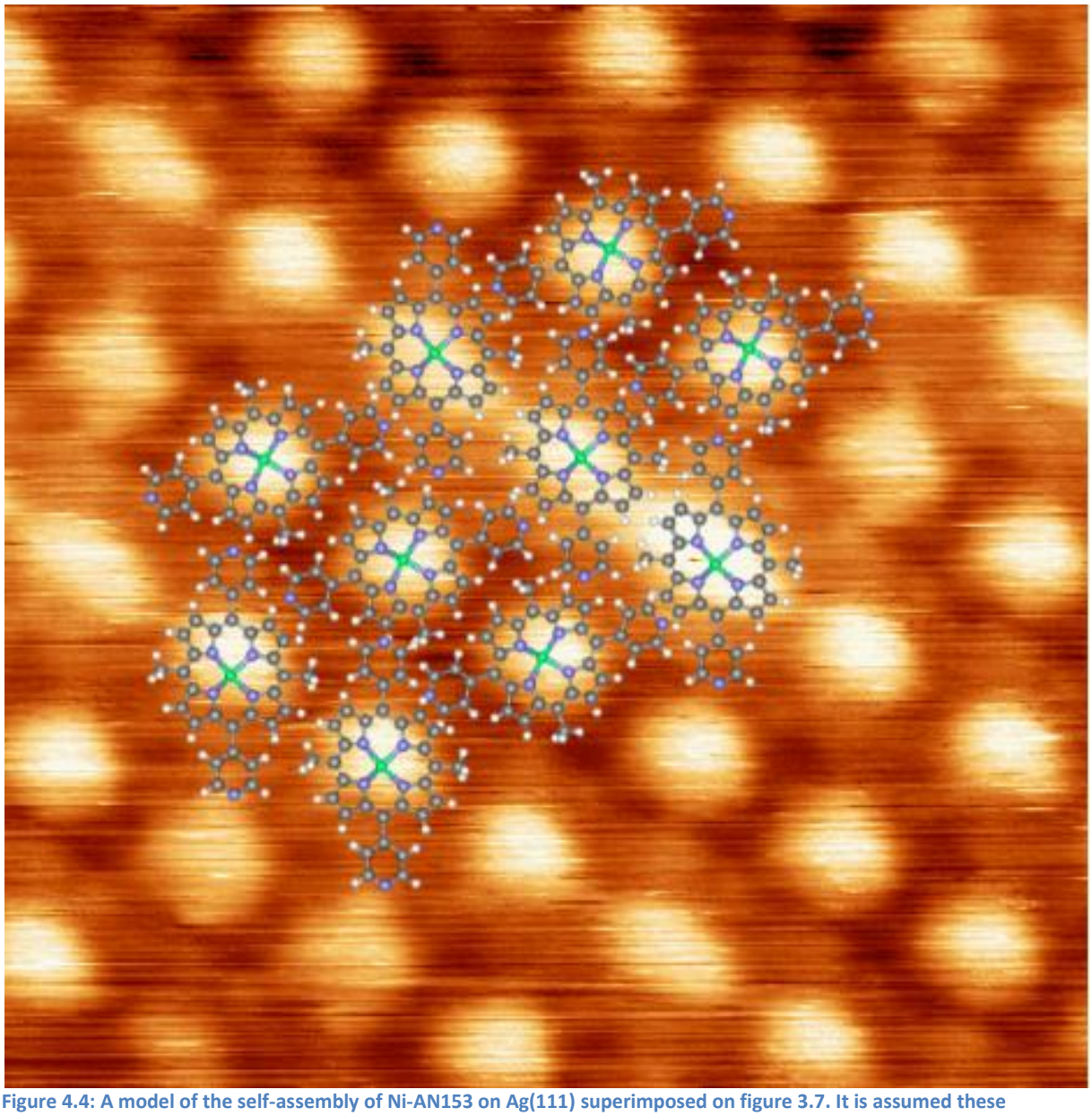

Figure 4.4: A model of the self-assembly of Ni-AN153 on Ag(111) superimposed on figure 3.7. It is assumed these molecules bind through hydrogen bonding.

The second phase of Ni-AN153 was found after the deposition of cobalt (figure 3.5). It seems to be the same phase as 2H-AN153 after cobalt deposition (figure 4.2). Both are a 3-fold hexagonal network. It is assumed the dots that can be seen in figure 3.7 are actually 3 pyridyl groups binding to 1 cobalt atom. As 1 bonding site is used to bind the cobalt to the surface all 4 of the bonding sites of cobalt are used in this network. A model of this network based on a zoom of figure 3.5 is shown in figure 4.5.

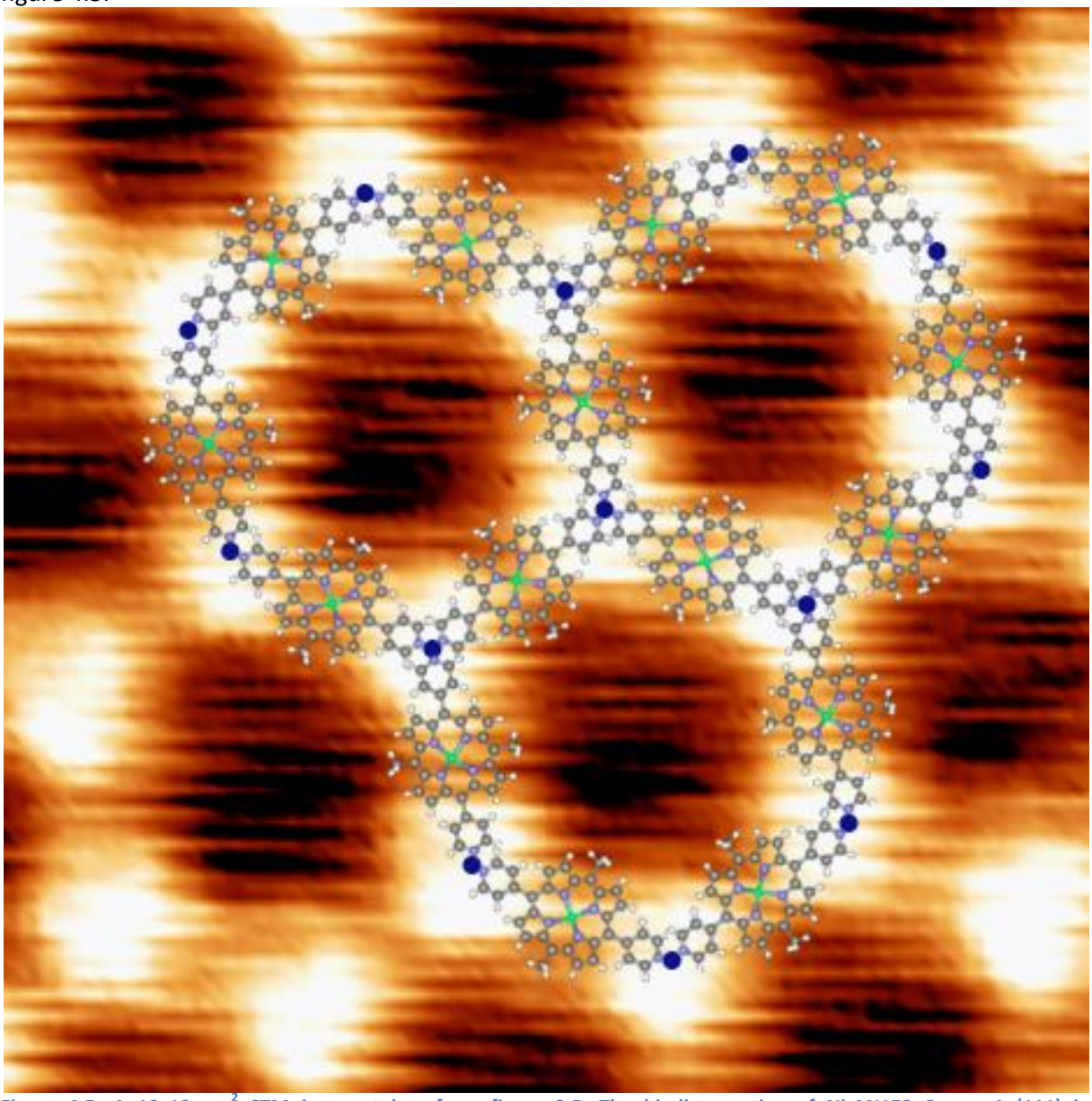

Figure 4.5: A 10x10 nm^2 STM image, taken from figure 3.5. The binding motive of Ni-AN153+Co on Ag(111) is superimposed upon the STM image. The cobalt atoms are shown as blue dots and assumed to bind to 3 pyridyl groups, each belonging to one Ni-AN153 molecule.

The last phase observed was after annealing the Ni-AN153+Co sample at 200°C. This network is shown in figure 3.8. For the unit cell of this assembly the parameters a and b, respectively along lines A and B, as shown in figure 3.8 are:

a=1.20 nm
b=1.49 nm
ϕ=90°

Table 4.4: unit cell parameters for the network of Ni-AN153 on Ag(111) after cobalt deposition and annealing.

The size of the molecule is approximately 1.6 nm, from pyridyl group to pyridyl group, by 1.8 nm, for the span of the hexyl chains. From this size it is assumed that the hexyl chains come down onto the surface and are placed next to each other, causing the distance of 1.49 nm between molecules in the b direction. In the a direction the distance is less than the size of the pyridyl groups, so it is assumed that these groups are rotated slightly and are placed next to each other. A model of this network, based on the STM image shown in figure 3.8 is given in figure 4.6.

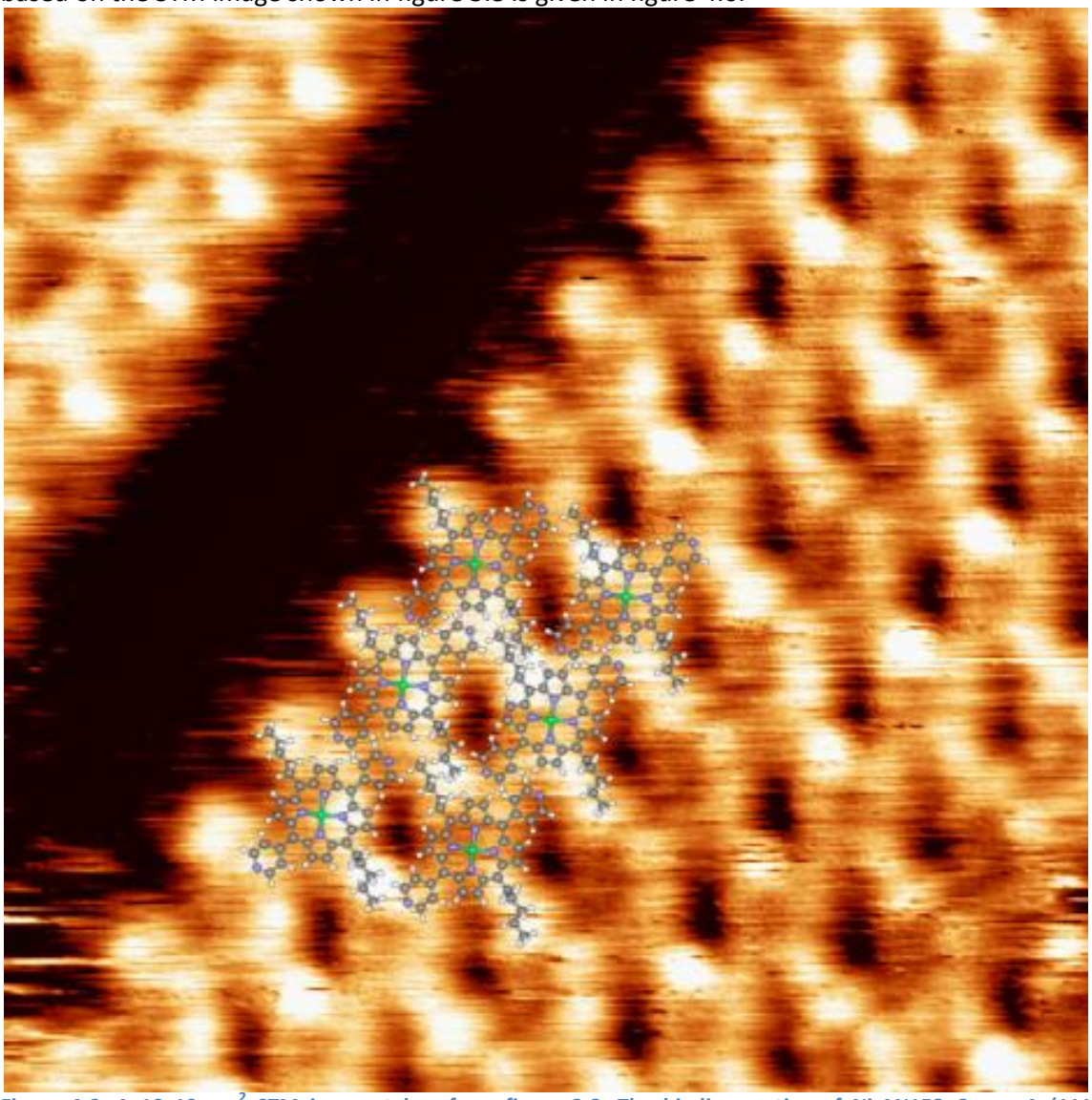

Figure 4.6: A 10x10 nm^2 STM image, taken from figure 3.8. The binding motive of Ni-AN153+Co on Ag(111) after annealing is superimposed upon the STM image.

From the model it cannot be derived whether the pyridyl groups bind through H-bonding or cobalt interaction, as N-H binding is about the same size as the metal coordinated bonds. To determine the chemical environment of cobalt a XPS measurement of the cobalt is done. It is however unlikely for the cobalt to form 3 bonds, 2 to the pyridyl groups and one to the surface, as this would mean there is still one free binding site left on the cobalt.

4.3) XPS analysis

4.3.1) Nickel $2p_{3/2}$

The values of the nickel peaks before and after annealing are very close to each other The annealing made a difference of -0.1 eV. It can therefore be assumed the chemical status of the nickel did not change due to the annealing.

When the chemical shift values, compared to metallic nickel, of 1.7 eV and 1.6 eV are compared to previous research[20] of metalized porphyrin, it can be concluded that this chemical shift coincides with a nickel binding to the core of a porphyrin molecule. It can therefore be assumed the nickel stays within the AN153 core before and after the annealing.

4.3.2) Cobalt $2p_{3/2}$

Following the previous research on 2H-AN153 an XPS analysis of the molecule was done. the resulting spectra of cobalt outside and inside the 2H-AN153 core are given in graph 4.1. It can be seen that the cobalt binding into the core appears as a second peak next to the peak for metallic cobalt, as shown in black.

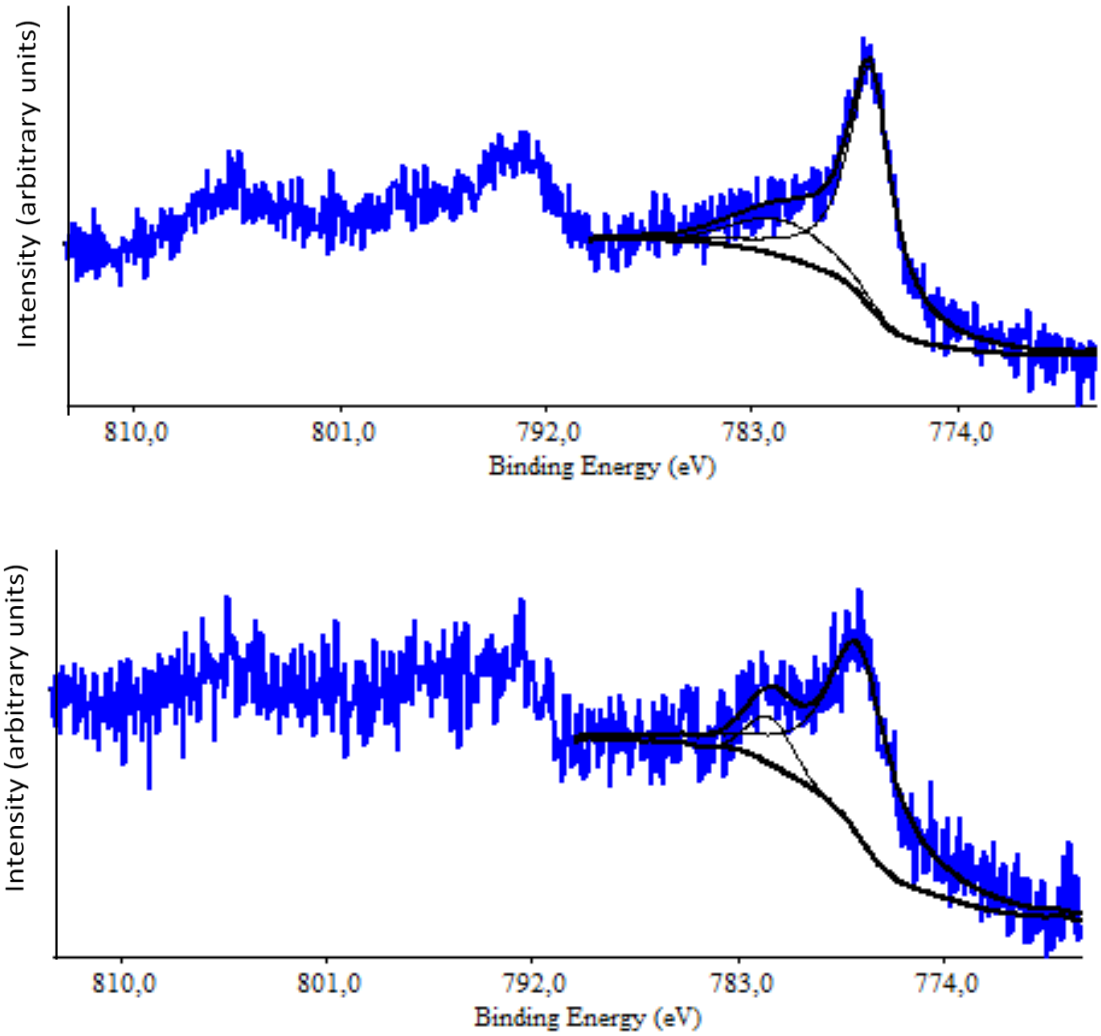

Graph 4.1: Comparison of cobalt $2p_{3/2}$ XPS spectra inside and outside 2H-AN153 network. Top: cobalt outside the 2H-AN153 network . Bottom: cobalt inside 2H-AN153 network[19].

The values found for the XPS peaks of cobalt in Ni-AN153 suggest the cobalt remains outside the molecule core for three reasons. Firstly for the cobalt the difference in the chemical shift before and after annealing is -0.3 eV. This is a small difference and suggests the cobalt did not change phase during the annealing. Secondly the chemical shift compared to metallic cobalt both before and after annealing is small, -0.2 eV and -0.5 eV respectively. This small change suggests the cobalt does not occupy the core. Thirdly, when the cobalt spectra of Ni-AN153 are compared to the cobalt spectra of 2H-AN153 no second peak is was found as is the case with cobalt binding into the 2H-AN153 core.

From the shift of the cobalt peak it cannot be concluded whether the cobalt binds to the pyridyl groups after annealing or stays in a free metallic state.

5) Conclusion

A porphyrin derivative molecule named AN153 was deposited on Ag(111). From previous research it is known that the molecule forms a close packed network. It is also know that when cobalt is added the molecules bind to the cobalt, through their pyridyl groups, to form a 3-fold hexagonal network. When the sample is than annealed it again becomes a close packed network.

In this research AN153 was used with a core that was metalized with nickel. This Ni-AN153 forms a close packed network similar to the network observed with non metallic AN153 (2H-AN153) after cobalt deposition and annealing. When cobalt is added to the Ni-AN153 a second phase exists besides the initial phase. This second phase is similar to the 3-fold hexagonal phase that was observed with 2H-AN153 when cobalt was added. When the sample gets annealed a new phase appears. From the STM data it cannot be concluded whether this phase is stabilized through hydrogen bonding or i metal-coordination.

XPS results showed that both nickel and cobalt do no exchange upon annealing Thus nickel stays inside the porphyrin core and cobalt stays outside the core. Therefore, for the latter phase, the Ni-AN153+Co after annealing, it still cannot be concluded whether cobalt is binding to the molecule.

Future research should be done in order to find out if the network that Ni-AN153+Co forms after annealing is metal coordinated or hydrogen bonded. Another way to change the symmetry of the sample is to change the substrate. During this research Ag(111) is used, however on other surfaces the molecule is expected to act differently as the lattice constant of the substrate changes. Another focus is low temperature STM in order to reduce the thermal energy, causing the molecules to have less energy to diffuse on the surface.

6) List of abbreviations

2H-AN153: The non metalized form of the porphyrin derivative molecule AN153, in which 2 hydrogen atoms occupy the core.
Ni-AN153: The porphyrin derivative molecule AN153 with a core that is metalized with nickel.
Ni-AN153+Co: The porphyrin derivative molecule AN153 with a core that is metalized with nickel and where cobalt is deposited on the molecule.
STM: Scanning tunneling microscopy
UHV: Ultra high vacuum
XPS: X-ray photoelectron spectroscopy

7) References

1) S. Rovira (2005), *Tinned surface in Spanish Late Bronze Age sword,* Surface Engineering, Volume 21, Issue 5-6, pp. 368-372
2) G. Binnig, H. Rohrer (1986). *Scanning tunneling microscopy*, IBM Journal of Research and Development **30**: 4
3) Johannes V. Barth (2009), *Fresh perspectives for surface coordination chemistry,* Surface Science 603 1533–1541
4) Johannes A. A. W. Elemans, Shengbin Lei, and Steven De Feyter (2009), *Molecular and Supramolecular Networks on Surfaces: From Two-Dimensional Crystal Engineering Reactivity*, Angew. Chem. Int. Ed. 2009, 48, 7298 – 7332
5) S. Stepanow, Nian Lin, Johannes V Barth (2008), *Modular assembly of low dimensional coordination on metal surfaces,* J. Phys.: Condens. Matter 20, 184002 (15pp)
6) Sybil P. Parker, *The McGraw-Hill Dictionary of Scientific and Technical Terms,* New York, McGraw-Hill Professional
7) P. Hofmann (2005), *Lecture Notes on Surface Science*, Århus University version 2,5.
8) Repairfaq.org*, Turbomolecular Pumps and Drag Pumps: Technical Notes,* http://www.repairfaq.org/sam/vacuum/tmpnotes.htm
9) T. Banerjee (2014), *Nanofabrication and Nanoprobing: Lecture VI.*Rijksuniversiteit Groningen
10) Nobelprize.org (1986), *Press Release: The Nobel Prize in Physics 1986,* http://www.nobelprize.org/nobel_prizes/physics/laureates/1986/press.html
11) C. Julian Chen (1993), *Introduction to Scanning Tunneling Microscopy,* New York, Oxford, Oxford University Press.
12) Institut für Angewandte Physik Wien, *The Scanning Tunneling Microscope,* http://www.iap.tuwien.ac.at/www/surface/stm_gallery/stm_schematic
13) a: Pardue University: Department of Physics and Astronomy, *TEM Pictures of STM Tips,* http://www.physics.purdue.edu/nanophys/uhvstm/tip.html;
b: Royal society of chemistry, *Experimental nanoscience for undergraduates,* http://www.rsc.org/Education/EiC/issues/2008Mar/ExperimentalNanoscienceUndergraduates.asp
14) Oxford Instruments, *VT SP,* http://www.omicron.de/en/products/variable-temperature-spm/instrument-concept
15) J. C. Vickerman and I. S. Gilmore (2009), *Surface analysis: The principal techniques*, John Wiley and Sons Ltd.
16) Los Alamos National Library, *XPS Work,* http://www.lanl.gov/orgs/nmt/nmtdo/AQarchive/04summer/XPS.html
17) I. Horcas et al. (2007) Rev. Sci. Intrum. 78, 013705
18) J.F. Moulder, W.F. Stickle, P. E. Sobol, K. D. Bomben, *Handbook of X Ray Photoelectron Spectroscopy: A Reference Book of Standard Spectra for Identification and Interpretation of Xps Data*, Eden Prairie (MN), Perekin-Elmer Corporation, Physics Electronics Division.
19) F. Studener, Personal communication.
20) S. A. Krasnikov, N. N. Sergeeva, M. M. Brzhezinskaya, A. B. Preobrajenski, Y. N. Sergeeva, N. A. Vinogradov, A. A. Cafolla, M. O. Senge, A. S. Vinogradov; *An x-ray absorption and photoemission study of the electronic structure of Ni porphyrins and Ni N-confused porphyrin*, J. Phys.: Condens. Matter 20 (2008) 235207 (6pp)